Towards A Standard Approach For Future Vertical Axis Wind Turbine Aerodynamics Research and Development

Andrew Barnes*, Daniel Marshall Cross, Ben Richard Hughes

Mechanical and Aerospace Engineering, University of Strathclyde

Abstract

The development of Vertical Axis Wind Turbines (VAWTs) has continued for nearly half a century without agreement on a valid procedure for the design and testing of turbines, and it is clear that this has had an impact on the ability to bring a VAWT to commercial success. This has largely been due to analysis methods for their complex aerodynamics being either insufficiently accurate, or having very high computational time requirements, or the high costs attached with experimental testing. It has also been impacted by the previous conclusion that Horizontal Axis Wind Turbines (HAWTs) were simply the better option which has resulted in reduced investment into VAWT development. Computational Fluid Dynamics (CFD) analysis has now become the most common, allowing for a considerable increase in the amount of research that can be produced and enabling analysis of farm configurations, which has shown increases in efficiency, to the opposite of HAWTs. Many examples can be found which demonstrate complete disagreement between literature, and so this review has critiqued available articles and reports to create a consensus on how to test and design VAWTs from an aerodynamic perspective accurately and effectively. Recommendations for testing methodology, turbine and farm design have been produced.

Word Count: 11,547

Keywords: VAWT, Review, CFD, Aerodynamics

*Corresponding Author Details: andrew.barnes@strath.ac.uk

Nomenclature

C_p	Power Coefficient
C_{AP}	Array Power Coefficient
$C_{p\text{-}max}$	Maximum Power Coefficient
C_N	Normal Force Coefficient
C_T	Tangent Force Coefficient
C_l	Lift Coefficient
C_d	Drag Coefficient
TSR	Tip Speed Ratio
C_m	Moment Coefficient
TSR_{opt}	Optimum TSR
ALM	Actuator Line Model
ADM	Actuator Disc Model
VTM	Vorticity Transport Model
CFD	Computational Fluid Dynamics
VAWT	Vertical Axis Wind Turbine
HAWT	Horizontal Axis Wind Turbine
CAWT	Cross Axis Wind Turbine
ρ	air density (kg m^3
V	Velocity (m s^{-1})
V_{hub}	Velocity at hub height
V_{avg}	Average Velocity
V_{ref}	Reference Velocity
V_{e50}	50 year extreme wind speed
V_{e1}	1 year extreme wind speed
V_{gust}	Change in wind speed due to gust
V_{cg}	Change in velocity due to extreme coherent gust
λ_1	Turbulence scale parameter
P_R	Wind Speed Raleigh Distribution
z	height (m)
z_{ref}	Reference height
a	boundary layer coefficient
I_{ref}	Reference turbulence intensity
b	turbulence coefficient
ϑ	Direction change
ϑ_e	Extreme direction change
ϑ_{cg}	Direction change from coherent gust

β	Parameter for Extreme direction change model
S	Swept Area (m^2)
TKE	Turbulent Kinetic Energy
Re	Reynolds Number
D	Diameter
σ	Solidity
AR	Aspect Ratio
t\c	Thickness-to-chord ratio
σ_1	Standard Deviation
S-A	Spalart-Allmaras
LES	Large Eddy Simulation
DES	Detached Eddy Simulation
MGM	Modulated Gradient Model
RANS	Reynolds Averaged Navier-Stokes
URANS	Unsteady Reynolds Averaged Navier-Stokes
DMST	Double Multiple Streamtube

1. Introduction

The focus on renewable and sustainable energy development due to the pressing issue of protecting the environment and its resources necessitates spreading research priority over a wide variety of technologies, not just those within the mainstream. Within the field of wind energy is one of the clearest examples of this with a renewed interest into Vertical Axis Wind Turbines (VAWTs), a technology previously considered disproven in favour of a competitor, Horizontal Axis Wind Turbines (HAWTs). This has allowed for the discovery of performance increases for VAWT arrays, in contrast to decreases in HAWT arrays. This issue remained untested during original development due to the high cost of creating multiple large scale prototypes for field testing and optimising spacing, combined with the relatively poor accuracy of analysis methods.

Newer research into VAWTs has been inconsistent however, with little consensus regarding testing and design methodology. While some research uses original data from the older Sandia reference turbines[1], this design is not compatible with some significant advances in VAWT research such as pitch control. Some articles reference newer H-turbine based results however these use small scale turbines which may not be applicable for utility scale[2].

The methodology is also variable, with wind tunnel and field testing unavailable to many researchers, rapid numerical analysis methods lacking accuracy under many conditions, and Computational Fluid Dynamics (CFD) methods showing contrasting validations. The small scales used for modern VAWT testing, alongside inconsistent validations, results in there being areas for improvement in guidelines for testing, and as a result of the incomparability caused, poor guidelines for design too.

In an attempt to collate the information available, a review of VAWT design has been conducted, which has been separated into 3 levels: turbine, blade, and farm. Then a review of testing methodology has been conducted which covers the different methods of analysis, conditions used, and CFD best practice.

1.1. Assessing VAWT performance and design

Similar to any energy related device the main performance criteria for VAWTs is efficiency. This is described by C_p, the power coefficient, defined by equation 1.

$$C_p = \frac{PowerOutput}{\frac{1}{2}\rho V^3 S} \tag{1}$$

For all wind turbines a maximum C_p of 0.593 is possible according to Betz's law [3]. In practice lower values are expected.

The array power coefficient can also be used, C_{AP}, which measures the average efficiency in an array. This is largely affected by farm design and wake velocity recovery.

The second major characteristic is the TSR/C_p curve shown in Figure 1 which denotes the relationship between Tip Speed Ratio (TSR or λ) and efficiency. The TSR/C_p curve describes both the maximum efficiency and the operating range.

The TSR/C_p curve can be divided into sections of Low, Optimal, and High TSR. For example investigation of self-starting behaviour considers performance at low TSR as some turbines will have negative C_p in this region, preventing self-starting. These are also used to compare simulation and experimental accuracy.

A third major characteristic is the torque ripple in Figure 2, this is the variation of torque for either the turbine or a blade across the azimuthal

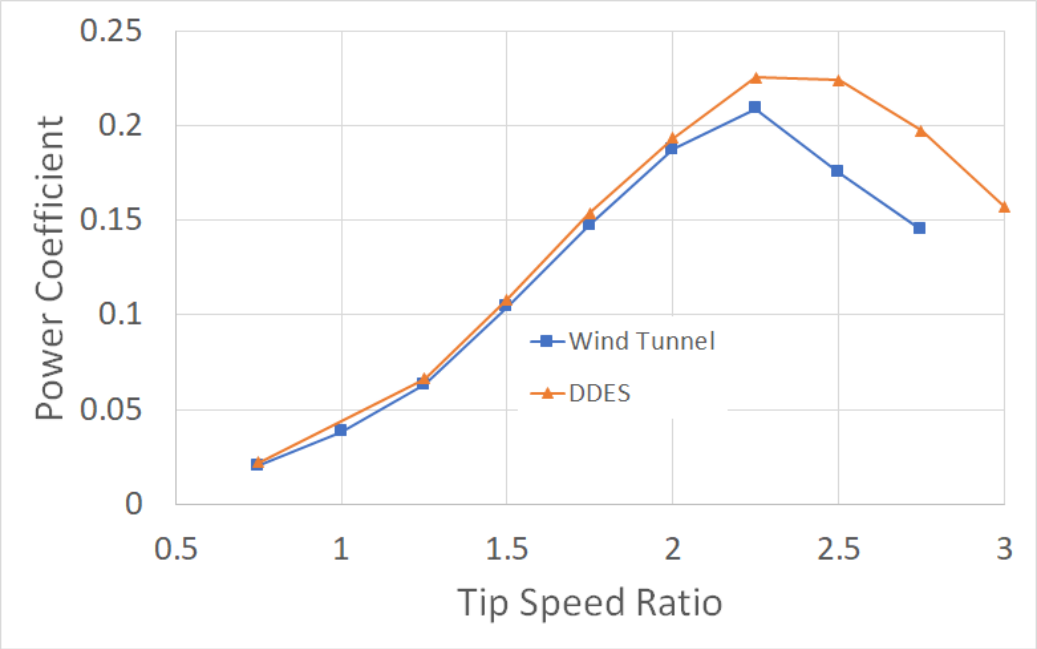

Figure 1: Example of a TSR/C_p curve comparing experimental and DDES CFD results [4]

range. This is commonly expressed as a torque rose, where the ideal shape is a circle which represents zero torque ripple.

For design there are non-dimensional measures in the form of solidity, blade Aspect Ratio (AR), and turbine AR. Solidity is a measure of the ratio of the area of the blades compared to the area of the turbine in a horizontal plane, defined by equation 2, where N is number of blades, c is chord length, and r is turbine radius. Blade AR denotes the ratio between the blade length (l) and chord in equation 3, while turbine AR in equation 4 shows the ratio between turbine height (h) and either turbine radius or diameter (D) depending on the source.

$$\sigma = \frac{Nc}{r} \tag{2}$$

$$BladeAspectRatio = \frac{l}{c} \tag{3}$$

$$TurbineAspectRatio = \frac{h}{r} \; or \; \frac{h}{D} \tag{4}$$

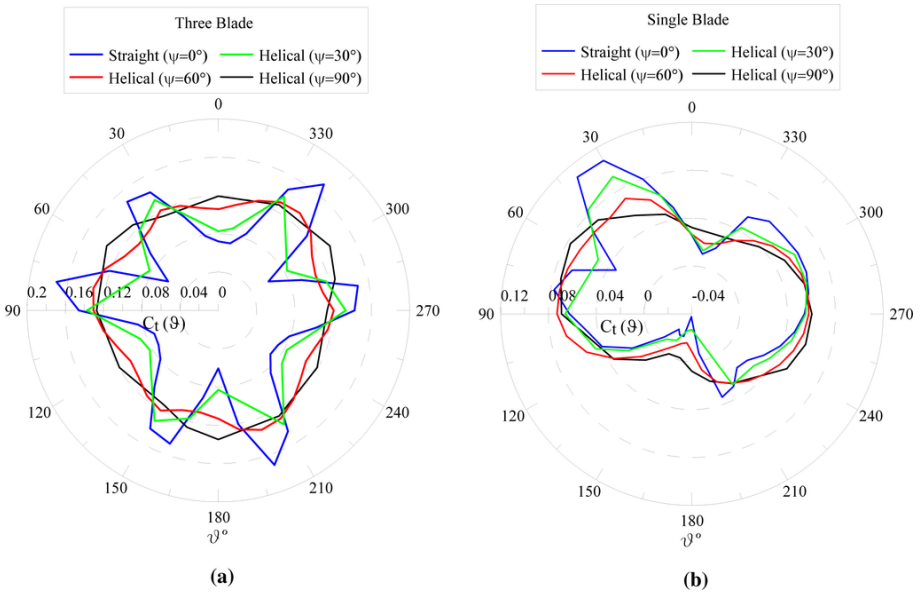

Figure 2: Example of a Torque Rose for Straight and Helical VAWTs [5]

Additionally, the choice of aerofoil and blade design can impact the performance of a VAWT.

2. Design

The design of a VAWT circles around three major passive features, namely the aerofoil, solidity, and blade design. Furthermore there are other passive and active features to be considered in more complex turbine designs which increase power production.

2.1. Turbine Design

2.1.1. Solidity and Number of Blades

Liang found that chord has a different relationship with C_p compared to the other variables in solidity (equation 2): number of blades and turbine radius, which have very similar relationships shown in figure 3 [6]. This may partly be due to the corresponding change in Re with chord length, however the turbine used is modelled on the one used by Fiedler[7] which demonstrates Re independence, and the magnitude of variation from the other conditions is much larger than expected from Re dependence.

$$Blade\ Density = \frac{N}{r} \tag{5}$$

From this result, the measure of solidity should be altered to improve comparability between turbines. Equation 5 should be used, and accompanied by chord length as an independent variable. As this hasn't been implemented in most literature, this section will continue based upon the original solidity definition.

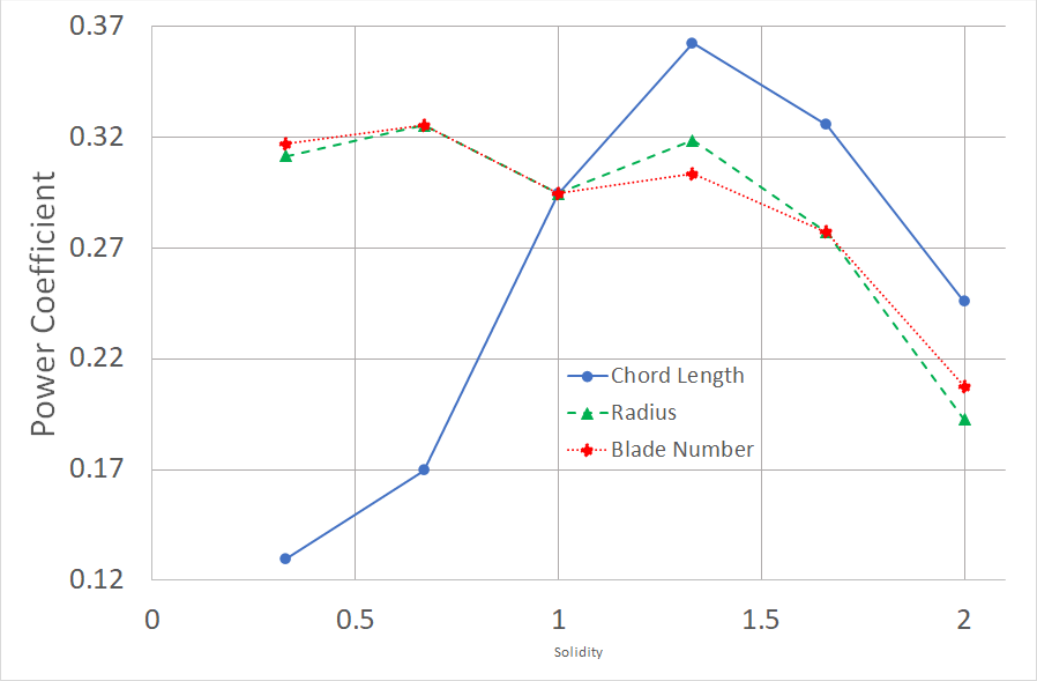

Figure 3: Comparing the effects of solidity as a function of chord, blade number, and turbine radius on performance [6]

Liang also finds that ideal solidity range depends upon scale, with larger scale turbines having a smaller ideal range of 0.2-0.6 whilst for smaller turbines it's 0.2-1.28[6]. Meanwhile Sagharichi suggests a range of 0.4-0.6 for fixed pitch VAWTs, however for variable pitch VAWTs even higher solidities of 0.8 offer better performance, particularly at lower TSR[8]. Hand found an ideal range of 0.2-0.4 with $C_{p\text{-}max}$ occurring at a solidity of 0.275[9]. The cause of the lower suggestion by Hand is likely due to the much higher Reynolds numbers tested, in the 10^6-10^7 range compared to 10^5 for Liang

and Sagharichi. Resultantly, a negative logarithmic relationship between optimum solidity and Reynolds number is expected, however further modelling is required.

Gosselin[10], Rezaeiha[11], Sagharichi[8], Blackwell[12], and Howell[13] demonstrate that higher solidity is suited to lower TSR operating conditions, with solidity increases causing decreases in TSR_{opt} and improving low TSR performance, while decreasing high TSR performance.

Jain demonstrates that increasing solidity via increasing chord length or number of blades improves $C_{p\text{-}max}$ at lower TSR, and increases blade power ripple[14]. Lee agrees on chord length and shows a smaller operating range[15].

Mohamed[16] and Claessens[17] both agree that increasing solidity aids self-starting behaviour however they disagree about the value required, with Mohamed stating >0.25 is sufficient while Claessens states >0.6. De Tavernier[18] confirms that aerofoil choice affects optimum solidity, explaining the discrepancy.

Both Battisti[19] and Sutherland[20] recommend using 3 blades instead of 2 with Battisti finding C_p increases across the TSR/C_p curve. Sutherland suggests the 3rd blade due to the reduction of torque ripple and ability to use a smaller tower, which reduces costs.

Mohamed[16], Gosselin[10], and Hand[9] demonstrate that an optimum solidity exists for maximising C_p. Hand shows that increasing solidity decreased $C_{p\text{-}max}$ compared to the optimum solidity of 0.275, while decreasing solidity also reduced $C_{p\text{-}max}$ but improves high TSR performance. Rezaeiha found that the choice of TSR can change the optimum solidity[11].

2.1.2. Reynolds Number

The consensus finds performance improvements with increasing Reynolds number (Re) [10][12][19][21][22][23][24][25] with evidence that there is a limit where Re independence occurs[12][26][27][28]. Re positively correlates with $C_{p\text{-}max}$ and expands the operating range due to improved performance at high TSR, therefore VAWTs are less effective in an urban environment due to their small scale and low wind speed causing low Re.

2.1.3. Aspect Ratio (AR)

From the early Sandia experiments it was known that increasing AR is the simplest way to increase power production of a VAWT as it doesn't impact other aerodynamic design characteristics[20]. AR is split into Turbine and Blade ARs, with both covered here to show comparability.

Jain[14], Zanforlin[23] and Peng[29] have shown that increasing Turbine AR results in increased efficiency with up to 100% increases demonstrated by Peng. Gosselin[10] and Hand[9] also demonstrate that increasing blade AR positively correlates with efficiency however they disagree on the returns, with Hand showing insignificant increases in C_p beyond AR=10 while Gosselin finds a significant difference between AR=7 and AR=15. Discrepancies are likely due to unknown confounding variables. Both Turbine and Blade AR should be maximised, but traded-off against other design aspects.

Hezaveh's[30] testing on VAWT wakes demonstrated that low turbine AR slows wake velocity recovery, so array design is also affected.

2.2. Blade Design

2.2.1. Aerofoil Design

The aerofoil used can severely impact performance, however one design won't offer better overall performance. Aerofoils have different responses to wide angles of attack, meaning some are more resistant to dynamic stall and so have smaller torque ripples. Other characteristics of the aerofoil can affect the TSR/C_p curve, impacting TSR_{opt} and $C_{p\text{-}max}$ Reynolds number and therefore scale also alters the TSR/C_p curve of an aerofoil.

The main criteria for aerofoil design are thickness-to-chord ratio (t/c) and camber. Regarding camber, results tend toward a slight camber being advantageous with Asr[31], Danao[32], Claessens[17], Islam[33], and Ferreira[34] demonstrating ideal camber of less than 4% and typically <2%. Elkhoury[35] found that symmetrical aerofoils perform better which is surprising given the low Re used, as other studies with low Re generate cambered aerofoils[31][34]. Claessens also found that camber becomes undesirable with higher turbulence, which is important because turbulence in the field is higher than used in most studies.

Findings for t/c show larger t/c improving low TSR performance due to delayed stall at the expense of high TSR performance[10][33]. Very high t/c can cause decreased $C_{p\text{-}max}$ due to increased drag[32][33] and is also less desirable at higher turbulence intensities[17]. Asr[31] found higher thickness aerofoils possess better self-starting behaviour and Elkhoury[35] finds that

thicker aerofoils perform better in higher solidity turbines. Islam[33] considered the effects of leading edge radius and trailing edge thickness on the performance of a modified LS-0417 aerofoil. An increase in leading edge radius from 2.97% to 4% improved performance while also improving resistance to surface roughness, and decreasing the trailing edge thickness from 0.71% to 0% improved high TSR performance.

Different aerofoil series have been studied, although the typical option is the NACA 4 digit series as this showed good promise in early development and is easy to manipulate. Symmetrical versions are often chosen as the baseline[17][31][32][33][34][36][37], though cambered versions are also used[38]. Mohamed used NACA 6 series aerofoils with the NACA 63-215 and 63-415 offering the best performance[39].

Regarding other series, Mohamed[40] investigated S and FX series aerofoils, of which the S-1046 and FXLV152 showed $C_{p\text{-}max}$=0.4051 and 0.3576 from 0.2964 given by the NACA0018 baseline, however they also had increased TSR_{opt} of 8 and 7 compared to 6 for the NACA0018. These have very high TSR_{opt} values compared to other studies. Mohamed and Islam tested LS aerofoils, the LS(1)-0413[39] and LS-0417[33] respectively. Mohamed found that the LS(1)-0413 performed slightly worse than the NACA63-415 at low TSR but had a wider operating range due to improved high TSR performance. Islam found that the NACA0015 produced better results across the board compared to the LS, S, and NLF aerofoils. Parakkal investigated Joukowski aerofoils and found that some offered a C_p improvement compared to the baseline NACA0012 and NACA4312[38].

Custom aerofoils are summarised in Table 1 methods can improve performance. Some studies such as Claessens[17] and De Tavernier[18] demonstrate increased thickness which will improve structural performance.

2.2.1.1. Summary of Aerofoil Design.

Choice of aerofoil is dependent on other aspects of turbine design. Optimisation algorithms offer a good method of design, although potentially at a high time cost.

2.2.2. Pitch

Changing the angle of attack of the blade allows for reduction or prevention of dynamic stall at low TSRs where effective angle of attack is higher, and also by ensuring the blade is at the optimum pitch for maximum power

Table 1: Studies producing customised aerofoils for VAWTs

Author	Method	$C_{p\text{-}max}$	% Change	Notes
Claessens[17]	Selection	0.48	5%	
Islam[33]	Selection	0.3	20%	
Balduzzi[41] & Bianchini[42]	Virtual Camber	N/A	N/A	
Ma[43]	Multi-Island Genetic Algorithm		27%	
Carrigan[44]	Differential Evolution Genetic Algorithm		6%	Solidity co-optimised
Ferreira[45]	Genetic Algorithm	0.525	4%	
De Tavernier[18]	Genetic Algorithm	0.57	8%	
Bedon[36]	Bézier Curve	N/A	8%	
Chen[37]	Orthogonal Optimisation	0.46	15.5%	
Jafaryar[46]	Response Surface Methodology	0.18	14.2%	

extraction at a given rotational angle. This concept is demonstrated by effective velocity U in figure 4.

2.2.2.1. Fixed.

Most of the literature shows that small negative pitches, called toe-out pitch, improve performance [47][7][15][48] by up to 29% however there is variation on the degree recommended. Even between Fiedler, Rezaeiha, and Lee which all use the same aerofoil, there are large differences. Fiedler recommends -3.9 to -7.8 degrees while Lee and Rezaeiha showed agreement with an optimum of -2 degrees. The major difference between the turbines used by Fiedler and those used by Lee and Rezaeiha is that Fiedler's has a higher solidity, however this opposes Sagharichi's findings that fixed pitch ceases to improve C_p at higher solidities[8]. In context, Fiedler's results may be anomalous.

Asr showed opposing results with a small positive pitch of +1.5 degrees giving the optimal performance, however a cambered aerofoil was used[31]. Meanwhile Mohamed showed that for the LS(1)-0413, which is also cambered, a pitch of zero is ideal[39]. It can be concluded that the optimum fixed pitch

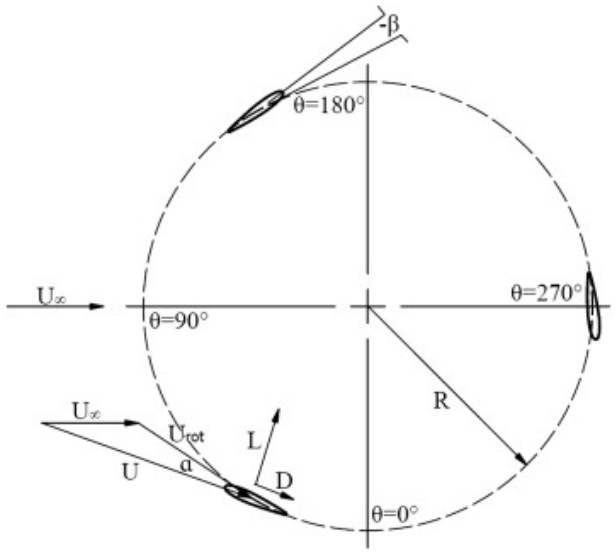

Figure 4: Diagram demonstrating pitch angle and effective angle of attack [47]

angle is dependent on aerofoil choice.

2.2.2.2. Pitching Axis and Mounting Point.

The mounting point of the strut on the blade causes an inherent toe-in or toe-out pitch, and so altering the mounting point has similar effects to a fixed pitch. Fiedler[7] finds that moving the mounting point forward resulted in an inherent toe-in pitch and so reduced C_p. In 2D simulations, Ferreira[34] shows that moving the pitching axis towards the trailing edge of the blade significantly reduced torque ripple while reducing C_p by <4%. In 3D however there was a 5% increase in C_p.

2.2.2.3. Variable.

Variable pitch mechanisms add complexity to the system but can improve power output and provide aerodynamic braking. The possible performance improvements are dependent on the control scheme as shown in table 2.

The sinusoidal[14][35] and eccentric[8] schemes are the simplest methods and can be implemented passively. Jain[14] only compared pitch amplitudes from 20 to 35 degrees and found that 20 degrees offered the best perfor-

Table 2: Comparison of Variable Pitch Control Schemes

Control Scheme	Fixed Pitch C_p or Annual Power (kJ)	% increase
Sinusoidal (Jain) [14]	0.25	44%
Sinusoidal (Elkhoury) [35]	0.18	39%
Eccentric (Sagharichi) [8]	0.33	33%
Target Angle (Gosselin, 2D) [10]	0.34	64.7%
Target Angle (Gosselin, 3D) [10]	0.19	63.2%
Genetic Algorithm (Paraschivoiu) [49]	-	30%
ANN (Abdalrahman) [50]	148kJ	39.8%
PID (Abdalrahman) [50]	148kJ	42.7%

mance, so a lower amplitude may be more desirable. Jain also investigated a variable amplitude method which would cater to varying TSRs to maximise performance during start-up and above TSR_{opt}.

Sagharichi[8] demonstrates that variable pitch has greater effects as solidity increases, particularly for turbines with more blades, and that torque ripple is reduced considerably using the eccentric scheme. Variable pitch also helps eliminate C_p dead-zones which will improve self-starting behaviour. Sagharichi also found a negative correlation between solidity and wake size using variable pitch.

Gosselin[10] uses a target angle of attack where the blades turn towards this angle during the upwind stroke and then towards the negative of this angle during the downwind stroke[10]. By using large angles of attack of 9 degrees the cost corrected C_p increased significantly while small angles of attack of 3 degrees resulted in a decrease of 26.4%. By using different target angles for upstream and downstream strokes, wake recovery can be improved at the cost of C_p decreasing by 0.03. Using a downstream angle of 18 degrees improved power ripple but caused worse wake velocity recovery.

Abdalrahman found that ANN offered a small advantage over PID due to its ability to model non-linearities, while both increased power compared to the fixed pitch reference[50].

2.2.3. Blade Shape

Numerous blade shapes have been proposed for VAWTs, aiming to improve performance, simplicity, or structural design.

2.2.3.1. Φ/Darrieus/Curved Bladed.

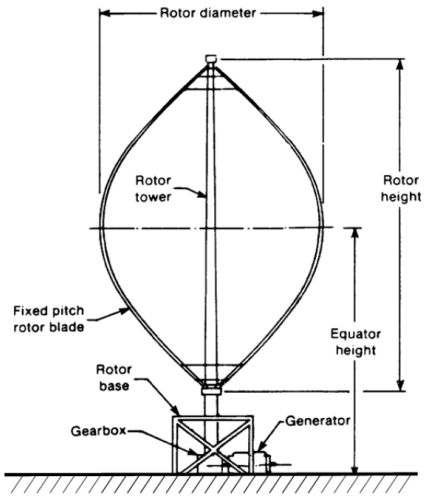

Figure 5: Diagram of a Darrieus Φ turbine [20]

The Φ design is the classical design used in Sandia testing[1] shown in figure 5. A curved blade design is used which should reduce blade tip effects however this comes with manufacturing difficulties. Compared to newer designs, longer blades are required for the same swept area, and the variable solidity has complex effects on performance. The blades must be either bent permanently into shape, which is a difficult process, or bent in place which reduces lifetime. Because of these issues the design became less popular, however some authors such as Delafin[51] continue to use it due to the experimental data available for larger scale Φ turbines.

2.2.3.2. H/Gyromill/Straight Bladed.

H-bladed turbines shown in Figure 6 are the most commonly evaluated in modern literature as they solve some issues of the Φ design while also offering greater simplicity. The design allows for evaluation using 2D CFD and the straight blades make manufacturing simpler. In this article, nearly all studies evaluated use H turbines unless stated otherwise.

Variations of H-turbines have been created such as variable geometry

versions which reduce the swept area at high wind speeds, and V-turbines which replace the tower with acutely angled struts.

Liu demonstrated using a Fluid Structural Interaction simulation that H-turbines with flexible blades increased $C_{p\text{-}max}$ by up to 8%, although performance reduces at higher TSR[52]. Many studies on H-turbines fail to account for this interaction.

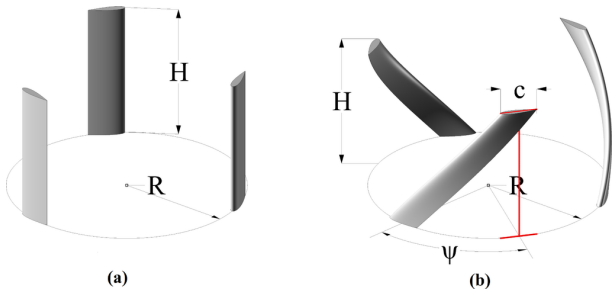

Figure 6: Left: H-Bladed VAWT, Right: Helical Bladed VAWT [5]

2.2.3.3. Helical/Gorlov.

Helical VAWTs, as shown in figure 6, use a blade which curves around the circumference of the turbine in order to reduce the torque ripple. Helical angle choice is important for using this design effectively, with low helical angles having minimal improvement on torque ripple or C_p[19][15], and that turbines with helical angles tending towards 360 degrees/number of blades offer a circle-tending torque rose[5]. Gosselin[10] demonstrates that a high helical angle reduces efficiency of the turbine, however this is likely due to the low turbine AR used which causes worse spanwise propagation of the separation bubble.

Battisti[19] and Scheurich[53] demonstrated better performance above TSR_{opt}, while Alaimo[5] found reduced $C_{p\text{-}max}$. Scheurich also demonstrated that helical turbines have improved resistance to unsteady conditions.

It should be noted that variable pitch is incompatible with helical turbines, so a design choice must be made.

2.2.3.4. Canted.

Armstrong investigated a turbine with canted blades, a design similar to helical turbines by allowing the blades to experience a variety of angles of attack at one orientation, however without curving the blade around the turbine circumference[47]. Armstrong used tilted blades which would affect results, however no other literature was found for canted blades. $C_{p\text{-}max}$ reduced from 0.32 to 0.29 when transitioning from straight vertical blades to canted tilted blades. Future work should investigate this design without tilting as it potentially offers some benefits of helical blades with simpler manufacturing.

2.2.3.5. Multi-section.

Multi-section turbines also propose to reduce torque ripple by splitting blades spanwise into staggered sections. Gosselin[10] found that while a 2-layered design reduces C_p ripple, C_p overall drastically decreases due to the low blade aspect ratio and wake interference between sections. This means that the design could be viable when a very high blade AR is used for each section. Solidity must also be considered as high solidity turbines cause greater wake interference between blades.

2.2.3.6. Variable blade profiles.

Hussain implements a variable aerofoil blade by stretching the NACA 63-415 airfoil thickness-wise, producing higher $C_{p\text{-}max}$ but a small operating range and higher torque ripple factor compared to constant thickness designs[54]. Other methods of varying blade profile such as swept blades could reduce tip effects. Using lower thickness-to-chord ratio aerofoils towards the top of the blades could improve the operating range by accounting for the spanwise variation of TSR due to atmospheric wind shear.

2.2.3.7. Summary of Blade Design.
Modern development should continue to focus on H-bladed derived designs, with future research focusing on canted blades and variable blade profiles which may offer simpler solutions compared to other designs.

2.2.4. Performance Enhancing Modifications

The performance of a turbine can be altered in other ways which often have a smaller impact on the overall design and may even offer cost effective upgrade pathways for operational turbines.

Samsonov[55] added small airbrake flaps of 0.01-0.05*S which had a considerable impact on C_p. Jet brake flaps have the best braking ability and the potential to considerably increase max C_p, without considerable power loss like air brakes[55].

Gurney flaps have been evaluated in several forms. Yan used a single edged Gurney flap at the trailing edge which reduced TSR_{opt} and increased $C_{p\text{-}max}$. The height of the Gurney flap affects performance with a height of 3% of chord offering the highest $C_{p\text{-}max}$ until TSR>2.5. The relationship between height and performance between 2-4% of chord needs clarification[56]. Malael[57] used double edged Gurney flaps at the trailing edge, finding significantly reduced TSR_{opt} with a wider, but lower operating range. Zhu completed a comparison of two side, one side inboard and outboard, and equivalent dimple Gurney flaps[58]. The outboard and outboard dimple Gurney flaps offered the best performance with insignificant difference between them for lower solidity turbines. At higher solidities however, while $C_{p\text{-}max}$ is still higher than the clean aerofoil, high TSR>2.5 performance is often worse than the clean aerofoil. There is also a significant difference between the performance of the dimple and no dimple gurney flaps at higher solidity however the relationship is unclear.

The original Sandia tests investigated utilising Vortex generators to trip the boundary layer which would reduce the effects of dynamic stall, however no significant effect on efficiency was seen[20]. A leading edge rod design was proposed by Zhong[59] as an alternative to vortex generators showing a 31.7% increase in lift-to-drag ratio, however this was not implemented for a full VAWT and would require significant investment into its structural design, particularly regarding the flexibility of the rod its effects on aerodynamic performance.

Gosselin added end-plates to the blade-tips in order to reduce tip vortex effects, finding that a small aerofoil shaped end-plate resulted in a 10% increase in C_p while a large circular end-plate reduced performance due to increasing drag[10]. Jiang[60] used a similar aerofoil end-plate design but found small improvements in power output of up to 5.2%, with larger end-plates increasing efficiency, which questions whether Gosselin's hypothesis was correct. Jiang also found that moving the struts towards the end-plate resulted in further increases up to 10.48%. In contrast, Villeneuve[61] used

circular and semi-annular end-plates which cover the circumference of the turbine, a design also proposed by Gosselin, finding 33.1% and 20.6% increases in efficiency respectively. These are a simple device for improving performance however their increase in efficiency must be balanced against material costs, alongside effects on the turbine wake, particularly in a farm context. The circumference covering end-plates could also be used as struts which may further reduce cost of energy.

Winglets are a commonly utilised technology in modern aeroplanes due to the significant improvements in efficiency offered, and this has also been considered for VAWTs. Laín tested two winglet designs, finding that a symmetric raked wingtip could improve efficiency by up to 20%[62], while Zhang tested 25 different cases finding increases in C_p of up to 10.5%[63]. Zhang's testing found that a single blade case increased performance by up to 31%, demonstrating the importance of a full VAWT case for representative results. Designers and researchers will need to make a choice over whether to use winglets or end-plates, as the semi-annular and circular end-plates offer higher efficiency improvements, but their effects in an array context require analysis.

Leading edge suction slots were first investigated in VAWTs by Sasson[64] finding that efficiency improvements up to 150% were possible with a double suction slot design. Sasson's research was built upon by Rezaeiha[65], finding that a single suction slot could produce efficiency increases of up to 1134%, however this was highly dependent on turbulence intensity and TSR, with their testing using a higher turbulence intensity of 25% showing a more modest increase of up to 99%, occurring at TSR=2.5. Rezaeiha found that the performance improvements increase with TSR however their testing only goes down to TSR=2.5, so further testing is required for lower TSRs. If this trend continues at lower TSR then improvements in self-starting behaviour and low TSR performance would be seen, producing an overall more viable turbine design which allows self-starting and increased operating TSR performance.

Synthetic jet actuators serve a similar purpose to leading edge suction slots but allow for both suction and blowing. Zhu completed a CFD analysis with synthetic jet actuators showing a 15.2% increase in power coefficient compared to normal blades[66]. Given that synthetic jet actuators are placed closer to the trailing edge where there is still high vorticity in the leading edge suction slot blade testing by Rezaeiha, the combination of the two tech-

nologies may allow for a further combined increase in performance than each technology alone.

Mohamed[67] proposes a passive leading edge slot design, finding increases in C_p at low TSR giving improved self-starting performance but a lower $C_{p\text{-}max}$ and worse high TSR performance. Torque ripple is reduced in the downwind section at low TSR too. This design involves a large cutout from the blade, which occurs where most blades would contain their major stress bearing components including the spar and spar cap, so there would be significant implications for the structural design. These could be mitigated by using the slot in limited regions across the length of the aerofoil, for example at the ends of blades where load bearing is lower, however the aerodynamic implications would need to be reconsidered.

Qin[68] suggested that struts must be designed to minimise the high losses they caused. Elkhoury[35] showed that including struts in their simulation significantly reduced $C_{p\text{-}max}$ and caused a lower TSR_{opt}, however it was also shown that effects were negligible at low TSR (<0.75). Goude stated that Turbine Aspect Ratio should be balanced against the number of struts needed to meet structural design requirements because the introduction of an additional strut per blade would cause significant losses[69]. Hand studied strut design and produced aerofoil-shaped struts with a variable thickness-to-chord ratio (t/c) which would improve high TSR C_p[9]. Significant differences were found between t/c=0.12 and t/c=0.21 aerofoils with $C_{p\text{-}max}$ reducing by 0.01, and a further decrease of 0.05 when moving up to t/c=0.30. Effects of changing thickness below TSR<1.7 were negligible. Mendoza[70] found that pitching the struts can reduce turbine wake effects which can be used to improve array performance.

Wang investigates a serrated leading edge design which is biomimetic of whale fins[71]. Using a serrated edge resulted in C_p increases up to 18.7% with most improvement towards lower TSR, however no performance is lost at higher TSR. The wavelength of the serrations affects the TSR/C_p curve however no clear relationship was found with both wavelength=0.33c and 1.0c outperforming 0.67c, with the 0.33c condition having better performance below and around TSR_{opt}, while 1.0c has a higher $C_{p\text{-}max}$ and better performance around and above TSR_{opt}. This design would be more complex to manufacture, which would impact cost of energy. The effects of surface roughness due to debris collected over the turbine life cycle will also need to

be considered.

Zamani proposed J-blades to improve $C_{p\text{-}max}$ and self-starting behaviour, which was confirmed in their studies using 2D and 3D CFD[72][73]. However worse performance was found at high TSR (>2.5). It was also shown that wake velocity recovered sooner. Pan[74] disputes these results, with overall reduced performance compared to conventional blades. J-blades also require investigation from a structural design viewpoint.

Howell tested a turbine with rough and smooth blades, finding that the surface roughness had an impact on performance which varied with wind speed. At lower wind speeds performance reduced with smoothing while performance improved at higher wind speeds, particularly at high TSR[13]. Therefore regular cleaning or coatings which reduce deterioration of surface roughness are required to avoid performance losses with age.

An alternative take on aerofoil-based struts is the Cross Axis Wind Turbine (CAWT) design by Chong[75] which attempts to create additional power from struts. Deflectors or tilting of the turbine are used to produce a more favourable flow direction for the design, showing very large C_p increases of up to 131.6% compared to an equivalent VAWT with no deflector [75][76]. Wang showed that CAWT designs have reduced torque ripple and a higher TSR_{opt} compared to equivalent VAWTs[77]. This testing was conducted only at low TSR so further testing is required.

Guide vanes and stators offer a simple way to increase the swept area of a turbine and improve flow direction, thus improving power output significantly. Takao's[78] unidirectional guide vane increased power output by 80% while Nobile's[79] omnidirectional stator showed an increase of 35%. Zanforlin proposed a rooftop design with up to 50% power increase using a cowling, however they also found that raising the turbine by 1m to utilise boundary layer effects instead of using the cowling resulted in a 56.25% increase[80].

A hybrid Darrieus-Savonius VAWT proposed by Mohamed showed improved starting behaviour but very poor C_p otherwise with significantly reduced $C_{p\text{-}max}$ and a rapid decrease in efficiency at high TSR[16].

Strom proposed Variable TSR control as an alternative method to Variable Pitch control. Compared to fixed TSR this resulted in a 59% perfor-

mance increase using a semi-arbitrary control scheme and a 53% increase with a sinusoidal control scheme[81]. The scheme used results in very large, impractical changes in TSR across a rotation, with the TSR varying between 0.4-3.8.

3. Farms

As wind turbines are often clustered to take advantage of high wind speeds in a small area it is necessary to consider impacts of clustering. For HAWTs this involves minimising the distance between turbines while also minimising the effects of turbine wakes on following turbines[82]. Meyers[83] showed that a distance of 10D between HAWTs results in a power reduction of 40% compared to a turbine in the freestream. In contrast, Chowdhury shows that 9D is sufficient for complete recovery to freestream velocity for a helical VAWT[84] and so power reductions will be much smaller. Additionally this flow may have higher turbulence intensity which could even improve performance compared to isolated turbines[85]. Hezaveh finds that approximately 13D is sufficient for near complete recovery in some circumstances, with high solidity, high TSR, and intermediate to low turbine AR producing the fastest recoveries[30]. Other studies detailed in this section consider that VAWT farm design procedure could use other flow characteristics to increase power output. These studies are divided into those which consider small arrays, and large arrays which would be applicable to utility development.

3.1. Small Arrays

Zanforlin's closely spaced turbine pairs show improved performance compared to isolated turbines, with staggered outward counter-rotating turbines performing better than parallel or inward counter-rotating turbines[86]. They also showed in a separate study on Vertical Axis Tidal Turbines (VATTs) that a side-by-side configuration increases C_p by 0.09, and a triangular formation also increases $C_{p\text{-}max}$ although only by 0.03[87]. However the triangular configuration was less susceptible to severe power drops from adverse current direction. Ahmadi-Baloutaki found opposing results for counter-rotating pairs with a slightly decreased performance in a low intensity wind tunnel, but the triangular configuration resulted in considerable power output increase for the downstream turbine compared to the isolated conditions[85]. They also

found that the TSR/C_p curve was vastly differently for the downstream turbine, even when adjusted for turbulence intensity, so experimental validation may be required for downstream turbines in arrays.

Lam conducted wind tunnel tests for turbine pairs, and provides lateral and vertical velocity profile graphs which are useful as an experimental validation of turbine pairs[88]. Counter-rotating turbines offered the best results and showed much better wake velocity recovery. The wakes of the two turbines begin to merge together downstream, with a high velocity maintained in the middle between the turbines which begins to dissipate cross-stream until the wake merger. Use of inwards or outwards rotation will depend on the context of the turbines, where inward rotation is advantageous for closely-packed farms due to a smaller lateral wake, allowing for lateral spacing between pairs of 2.5-3D compared to 3-4D for outwards rotating pairs. Streamwise velocity reduction in the wake was greatest towards the mid-span of turbines, while the greatest cross-stream effects occurred towards rotation at the mid-span and against the rotation at the tips, with reduced effects at quarter-span. The greatest vertical velocity effects were at the tips with the velocity directed towards the mid-span on the outside of the turbine pair and away from the mid-span between the pair. De Tavernier's[89] pairs of co and counter-rotating VAWTs increased C_p from 0.55 to 0.58, with increasing solidity and TSR increasing C_p, confirming Lam's results[88].

Giorgetti found an efficiency increase of up to 10% using rotating pairs compared to isolated turbines, and a 4.4% increase for a 4 turbine array[90]. They also showed that wake structures produced by VAWTs cannot be recreated using rotating cylinders via the Magnus effect.

Brownstein[91] investigates the effects of wind direction on VAWT pair performance, finding that there is a region of approximately 50°where power output increases by an average of 14%, however the power output of the following turbine can decrease to zero when in the minimum velocity regions of the wake. The effects of wind direction reduce with greater spacing between the wind turbines. Given that the wind direction at most sites tends towards a given direction, arrays can be designed to maximise the time spent in a favourable direction and minimise time spent in an unfavourable direction. Further investigation is needed regarding larger spacing between turbines as Brownstein's largest spacing condition retained good performance while reducing the impact of unfavourable direction significantly.

Sahebzadeh[92] investigates the optimal configuration for dual rotor configurations, using CFD in contrast to the experimental method used by

Brownstein. They find a smaller increase in power output of 1.8% at an inter-turbine distance of 1.25D and angle of 75°. The pattern for the increase for the downstream turbine is similar with both studies demonstrating an increase providing the downstream turbine is situated sufficiently off-centre. However for the upstream turbine the results differ with Sahebzadeh only finding power increases when the turbines are parallel, while Brownstein finds increases when the downstream turbine is placed on the downstroke side for both co- and counter-rotating conditions, and a significant decrease on the upstroke side for the co-rotating condition. This difference is likely due to the differences in solidity, with Sahebzadeh using a low solidity turbine of 0.06 compared to 1.13 for Brownstein, which has been demonstrated to reduce the impact of arrays on performance by De Tavernier[89] and Barnes[93]

3.2. Larger Arrays

Due to the slower speed of simulating larger arrays there is less literature which can be applied to commercial scale farms. Whittlesey[94] proposed the 'School of Fish' design which could offer up to 40% improvements in turbine efficiency while Dabiri[95] expected that power per land area could be improved by a magnitude by using VAWTs instead of HAWTs. However, Dabiri failed to consider that very small spacing can be undesirable as the land around turbines is often used for other purposes, particularly agriculture. In practice there will be a case-by-case trade off between minimising the area required and maximising the use of that area. This is even more relevant for VAWTs due to their typically greater footprint over the land. Hezaveh found that clusters of 3 closely packed turbines provided the highest array efficiency in comparison to continuous aligned and staggered configurations with an increase of over 100%[96]. Barnes showed that the 3 turbine clusters of Hezaveh were a special case of the staggered configuration and that a closely packed staggered configuration offers the best array performance with power output increases of >80% compared to isolated turbines and up to 271.8% compared to the aligned configuration[93]. Barnes echoed De Tavernier's results[89] by showing that decreasing solidity may decrease the impact of array optimisation. Barnes also recommended the use of curved array designs in order to minimise the impact of unfavourable wind direction.

3.3. Mechanism of Improved Performance in Arrays

Several hypotheses for why VAWTs exhibit improved power output in arrays have been proposed. These mechanisms work together to create a combined effect. The virtual bluff-bodies of the turbines create an initial constriction[91][97] resulting in the Venturi effect[93][98][99] which increases the effective velocity on the blades and produces a more favourable wind direction upon the blades[86]. The vortical structures in the wake of the turbine then allow the constriction of the airflow and thus increased velocity to continue further downwind, hence resulting in increases in power output in a staggered configuration also[91][97]. The higher velocity in the constricted region as a result of the combined effect of two turbines also results in faster wake contraction[86][93][91].

3.4. Summary of Arrays

A clear advantage is seen from good array design, with closely spaced staggered designs offering greater power output and lower area use. The mechanism for increased power output in VAWT arrays is understood however further investigation is required to use this to design arrays.

4. Testing

In order to validate design choices, it is necessary to test their impact on performance. As with any area of engineering, tests can be conducted via either simulation or experiment. In general, simulation comes with a lower monetary cost though may involve a higher time cost, and allows for testing of impractical subjects. Experiments usually offer increased accuracy though this may not always be true if poor assumptions are made in the methodology.

4.1. Simulation

Several popular methods are available for simulating VAWTs, with most of these being based upon CFD, namely Streamtube, Actuator Line, and Vortex models. However there are also other Low Order models which do not require a CFD element. The Double Multiple Streamtube Model was one of the most commonly used during early years of VAWT development due to its reasonable accuracy and high speed with Vortex models appearing a few years later. Actuator Line models originally developed for HAWTs were

adapted for VAWTs in the 2000s. Recently CFD has become more viable so is now the most popular choice.

Bangga[100] conducted a study comparing the accuracy of several CFD software with several low order models. Low order models, particularly Improved Double Multiple Streamtube, often provided similar accuracy to the CFD models and sometimes were more accurate, however they performed worse in the high solidity condition. The comparable accuracy between CFD and low order models shown in this study may be due to lack of consensus on how to model VAWTs in CFD, and also the use of 2D CFD, as other studies have shown greater accuracy using CFD, which will be covered in section 2.1.5.

4.1.1. Low Order Models

Low order models enable faster simulation compared to CFD, however the simpler modelling can result in lower accuracy, or only be valid in limited circumstances. As these are widely covered by Islam[101], Jin[102], and Mohammed[103], they are summarised in table 3. Several other models have not been covered in previous reviews however so details are included below.

Table 3: Summary of Low Order Models

Model	Notes
Streamtube	Wind speed dependent[104][14][49][105][106]
Actuator Line Model	Closest model to full CFD[30][96][107]
Vortex	[108][109]
Cascade	[110]
Vorticity Transport Model	[111]
LLFWV	Includes Turbine Wake Modelling[112]
Hand Low Order	[9]
Tingey Reduced Order	[113]

4.1.2. Vorticity Transport Models (VTMs)

VTMs were developed originally for helicopters by Brown[114] then adapted for VAWTs by Scheurich[111]. VTM uses the Navier-Stokes equations in vorticity-velocity form to predict the wake, then uses aerofoil data to predict lift and drag, and thus power coefficient. Combining VTM with a dynamic stall model and strut corrections produces good predictions[111].

4.1.3. Lifting Line-Free Vortex Wake (LLFWV)

LLFWV is a more general method which can be utilised for both HAWTs and VAWTs with minimal adaptation. Turbine wakes can be predicted using this model which can also enable modelling farms with LLFWV. It is utilised by the open source application QBlade, where a validation by Marten found good agreement with CFD results[112].

4.1.4. Other Low/Reduced Order Models

Hand developed a Low Order Model in both 2D and 3D forms, where the 2D model shows reduced error of normal and tangential force coefficients (C_N and C_T) compared to S-A CFD and DMST models[9]. Very good prediction of C_p is shown using the 2D model until TSR_{opt}, while the 3D model continues to predict accurately until TSR>4.5. Tingey produced a Reduced Order Model which predicts wake velocity within 5-6% accuracy in milliseconds [113].

4.1.5. CFD

Due to the complex flow around VAWTs involving dynamic stall it is necessary to use an unsteady approach when completing CFD analyses. The flow shows a periodic nature which could allow for use of Periodic RANS which enables significantly faster analysis for appropriate flows. Campobasso found that simulating HAWTs with Periodic RANS had good accuracy and a time reduction factor of 6.5, but was unpromising for VAWTs due to a smaller time reduction factor and worse accuracy than Unsteady RANS[115]. It also highlights that incorrect selection of complex harmonics can result in very poor accuracy or slower analysis, meaning there is an additional layer to the verification process.

4.1.5.1. 2D vs. 3D.

The initial consideration in VAWT CFD is the use of a two- or three-dimensional domain, and this especially applies to H-VAWTs where the 3D design is an extrusion of a 2D design. A midway 2.5D approach is also available which uses a 3D model but only considers a section of the blades, with symmetry conditions applied to the walls at the ends of the section. Tip effects and struts, which can only be modelled in full 3D, have significant effects on VAWT simulation results however, with Castelli[116] and Hand[9] showing large decreases of up to 45% in C_p when these are accounted for.

Results overwhelmingly show that 3D offers better prediction than 2D, with very good predictions until high TSR and even then this is partly due to the simulated turbine lacking struts and shaft[13] as these have greater impact at higher TSR. An exception is Orlandi[117] which shows worse prediction of C_n and C_t compared to 2D, however this is likely due to the considerably reduced domain length and higher blockage ratio in their 3D simulation.

Li tested using 2.5D, where tip effects and struts are neglected, and showed that the differences from 2D for Unsteady Reynolds Averaged Navier-Stokes (URANS) modelling were negligible but significant differences were seen for Large Eddy Simulation (LES) modelling[118]. He[119] conducts a similar study but with a comparison to 3D simulations also. They show similar results with 2D and 2.5D URANS producing similar predictions while 3D URANS, 2.5D LES, and 3D LES produce similar results to each other and different to 2D and 2.5D URANS.

4.1.5.2. Turbulence Models.

Turbulence models are used to solve the gross effect of turbulence on the flow at the appropriate scale, in order to avoid Direct Numerical Simulation which is extremely computationally intensive. Two forms of turbulence modelling are commonly used: LES, which directly solves large scale eddies and uses a sub-grid scale model for smaller scale processes, and Reynolds Averaged Navier-Stokes (RANS) which uses the model at all scales, although some RANS models change behaviour near walls. As LES uses a more direct solving procedure it is usually more accurate than RANS, but at the cost of significantly greater computational requirements, so in cases where RANS models can provide sufficient accuracy these are used instead. Detached Eddy Simulation (DES) is an alternative which can be described as either LES with a wall model or hybrid LES/RANS depending on the setup. DES enables accuracy similar to or better than LES in appropriate circumstances, albeit with reduced time commitments. Furthermore, there is also Scale Adaptive Simulation (SAS), which aims to perform between RANS and DES.

It should be noted that LES and DES models require 2.5D or 3D analysis for good performance while RANS models do not so many studies which use RANS turbulence models use 2D analysis to reduce computational resource

requirements. As stated in the previous section, the choice of 2D, 2.5D, or 3D has a significant impact on the predictions, so the best performing turbulence models in 2D may perform poorly in 3D. Relatively high accuracy in 2D could even be an indicator of poor accuracy in 3D because large decreases in C_p are to be expected at high TSR when including tip effects and struts.

4.1.5.2.1. LES, DES, and SAS Models

Within LES models, Elkhoury[35] uses LES with a Smagorinsky sub-grid-scale model to validate C_p prediction against an experiment within a TSR range of 0.25-1.5. $C_{p\text{-}max}$ and TSR_{opt} are predicted accurately for all inlet velocities and aerofoils where both experiments and LES simulations were conducted. However for the $NACA63_4$-221 there was a small overestimation around $C_{p\text{-}max}$ demonstrating a need for case-by-case validation for CFD simulation of VAWTs, especially given that the experimental setups were the same in this study so the difference cannot be due to unknown factors.

Posa[120] considers wake prediction of an experiment by Howell[13] at TSR=1.35 and 2.21. Wake recovery was overestimated however this may be due to the small domain volume relative to the turbine resulting in blockage effects, which is evidenced by the freestream velocity being 5-10% greater than the inlet velocity. It should be noted that the experimental model uses an even smaller domain however, so this difference may be due to reduced blockage effects enabling greater recovery of the wake. The blockage effects also impact the Spanwise vorticity results, with the outer wake lines converging in the simulations further downstream while they continue to diverge in the experiment.

Li compares 2.5D LES against a URANS model, k-ω SST in 2.5D and 2D. 2.5D LES shows the most accurate prediction of C_p, C_l, C_d and C_m overall although there were some situations where 2.5D LES predicted less accurately [118]. Significant inaccuracies remained even with 2.5D LES however, which could be due to using the same mesh for LES and URANS simulations when typically a much higher cell count mesh is required for LES as this was not verified in the paper, or it could suggest that other methods such as 3D LES may be required for accurate analysis.

Different forms of DES are also used such as Delayed DES (DDES) and Improved Delayed DES (IDDES). An accompanying RANS model must also be chosen, with Spalart-Allmaras, k-ε, and k-ω being the most common.

Lei uses 3D IDDES with k-ω SST and compares against k-ω SST by itself alongside an experiment[121]. IDDES agrees very well with experimental C_p, overestimating by 2.89% at $C_{p\text{-max}}$ while k-ω SST underestimates C_p. At TSR=1.38 IDDES showed good prediction of wake velocity recovery while k-ω SST underestimates, however IDDES overestimates considerably at a higher TSR=2.478. Lei's study conducts a rudimentary mesh verification however with only two meshes considered, and the higher density mesh having only 25% more cells than the original mesh, but despite this a 1% increase in C_p was found, implying that there is a significant difference between the value found by Lei and the converged value. The geometry of the mesh also does not include the struts of the turbine which have significant effects on power coefficient[9][116]. The study does not include dimensions of the struts in the experimental turbine so it is difficult to determine whether the difference between the simulation and experimental results is within the expected range, although they appear to be cylindrical struts in the diagram which Hara[122] finds to cause much larger decreases in C_p than aerofoil struts, as considered by Hand[9], or no struts.

Lam[123] compared 3D IDDES with 2D and 3D simulations using the RANS model Transition SST, and an experiment by Tescione[124], finding that both 3D models had very good agreement with the experimental wake velocity while 2D estimated poorly. There was little overall difference in accuracy between the Transition SST 3D and IDDES 3D results, with Transition SST slightly more accurate for streamwise velocity and IDDES slightly more accurate for cross-stream velocity, however both demonstrate an offset from the experimental results on the upstream side of the turbine wake.

Dessoky[4] compared DDES-WENO with URANS-JST and an experiment by Li[25], finding that DDES-WENO predicted C_p well. Their URANS results overestimated C_p compared to DDES however it is unclear which turbulence model they used for URANS testing, so conclusions cannot be made that URANS approaches are overall less accurate. Their results also demonstrated that using a 3D simulation domain with matching dimensions to the wind tunnel domain was important to ensure comparability, as using a larger domain resulted in increases in C_p at higher TSRs.

Scale Adaptive Simulation for VAWTs has seen limited study, with Rezaeiha[125] providing the reference for its performance. In the study, SAS was compared against the Transition SST RANS model and SBES, a hybrid LES/RANS model, using 2.5D CFD. They found that the prediction from SAS was closer to SBES than RANS. It should be noted that while SAS did allow for a re-

duction by nearly half in mesh cell count and time per revolution compared to the hybrid LES/RANS model, the time per revolution was over 23 times higher compared to Transition SST so computational resource requirements remain prohibitive. There were still significant differences between predictions from SAS compared to SBES in some circumstances such as C_l and C_d so an argument for using hybrid LES/RANS models remains.

4.1.5.2.2. RANS Models

Amongst RANS models, the models commonly used in VAWT simulation are variants of k-ε, k-ω SST, and Transition SST. Several other models will also be covered.

A comprehensive comparison of RANS models was carried out by Rezaeiha[126], which considers 7 turbulence models: Laminar, Spalart-Allmaras, k-ε RNG, k-ε Realizable, k-ω SST, k-ω SSTI, Transition SST, and k-k_l-ω. Rezaeiha compares these turbulence models using a 2D CFD simulation against 3 experimental baselines covering leading edge circulation, turbine wake velocity, and C_p against TSR. The k-ω SST variants and Transition SST show the only good predictions with Transition SST performing best. No verification was shown for the meshes and a different meshing technique is used compared to Rezaeiha's previous VAWT papers where verification is shown[11][48][127][128] so it is indeterminable whether these results are representative of the converged results from these turbulence models. In some of the comparisons, only single rotation phase averaging is used due to computational resources required however this is unusual given the proportionately small additional resources needed for longer averaging.

A similar study was conducted by Daróczy[129] which tested 8 turbulence models covering the same models as Rezaeiha, with the exception of Laminar and k-ω SSTI, and addition of SAS and k-ε Realizable with standard wall treatment. SAS, k-ε Realizable with standard wall treatment, and k-k_l-ω were not used in the later testing however due to issues with convergence and stability. 2D CFD was used and the results are compared against 4 experimental baselines of C_p. It was found that Spalart-Allmaras, k-ε Realizable, and k-ω SST were the most accurate around TSR_{Opt} while all models were inaccurate at low TSR and overestimated at high TSR. In each of the comparisons, Transition SST overestimated TSR_{Opt} which was also seen in Rezaeiha's results[126] amongst other studies[8][26][28][130]. This study

demonstrates a rigorous verification process, considering 5 different meshes, all of the turbulence models, two different CFD software, and two TSRs in the verification. However there are deficiencies in their verification process, for example the lack of using Grid Convergence Index for determining mesh convergence[131] and a potential false plateau in domain size verification.

From these two comparison studies, k-ω SST is the only model which performs well in both. Further research is needed, including the use of more transparent and rigorous verification processes. Daróczy's study also does not consider wake prediction so can only be applied to C_p. Both studies use 2D simulation meaning their results cannot be applied to 3D simulations. They also utilise meshes with target y+ values of 1 in all scenarios, when Spalart-Allmaras and k-ε models allow for wall modelling which enables much higher y+ values of 30<y+<300 to be used which can reduce computational resource requirements. In order to address some of these issues and consider other aspects of the CFD results, more research must be considered and produced.

Almohammadi produced a similarly wide-ranging study including Spalart-Allmaras, k-ε RNG, k-ω SST, Transition SST, and Transition SST with Curvature Correction, however without comparing to an experimental baseline[132], although the setup is based upon an experiment by Bravo[133]. Instead of C_p which was investigated by the experiment, Almohammadi considered the separation bubble on the blades at 3 different angles of rotation. Blade position 1 inner and outer, alongside position 3 inner, represent an absence of separation bubble, and show recovery towards freestream velocity and beyond occurs at a shorter distance from the aerofoil surface with Transition SST models, followed k-ω SST, then k-ε RNG, and Spalart-Allmaras in that order. Positions 2 inner and outer, and 3 outer, show significant separation. Position 2 outer shows a similar relationship to above however the different turbulence models converge towards different velocities, and with k-ε RNG showing the greatest difference from the Transition SST results. For position 2 inner, the Transition SST models show much higher velocity. The other models show a reduction in velocity after reaching a peak while Transition SST models show a very slow recovery, with the curvature corrected version showing no clear recovery within the distance measured. Transition SST, k-w SST, and k-e RNG all converge to the same velocity with each showing an overshoot. For position 3 outer, k-ε RNG demonstrates the largest overshoot, followed by k-ω SST, then Transition SST. S-A and Transition SST with curvature correction show very different results with S-A appearing to

converge to a lower velocity, while the curvature corrected model shows no signs of convergence within the distance measured.

The lack of an experimental baseline prevents a conclusion being made about the overall accuracy of each model, although it can be determined that for situations where separation is limited or does not occur that there is little difference in accuracy between the models. However, the study can indicate the accuracy of a given turbulence model when used in conjunction with results from a sufficiently high resolution PIV experiment alongside a verified CFD simulation using one of the turbulence models used by Almohammadi. The very small distance of velocity measurement of 2.5% of chord used in the graphed data makes it difficult to compare results to most published experimental results which report separation bubble results using an image rather than comparable data points. While data could be extracted from these images, the accuracy of the extraction itself may be an issue, particularly at the distances used by Almohammadi which would often be sub-pixel scale. A suitable distance for measurement would be >30% of chord which would capture the full separation bubble under some circumstances, and potentially >150% of chord as shown by Buchner's experimental results.

4.1.5.2.3. Summary of Turbulence Models

Overall IDDES is the most accurate option however k-ω SST offers the best alternative where IDDES is not viable. Transition SST may have a small advantage over k-ω SST in some circumstances, though validation requirements are more stringent as will be explained in section 4.1.5.7.

4.1.5.3. Pressure-Velocity Coupling.

In most studies the SIMPLE Pressure-Velocity coupler is used as it is regarded as having the best performance for most applications. Lam[123] uses SIMPLEC alongside Li[118] with the justification that it offers faster convergence than SIMPLE and higher stability than PISO. Chowdhury uses PIMPLE which is a combination of PISO and SIMPLE that is available in OpenFOAM[84]. Several authors have done comparisons though they each leave out SIMPLEC and PIMPLE so these need further investigation.

Lanzafame found that PISO offered quicker convergence than SIMPLE and unlike Coupled predicted the wake accurately[134]. Contrastingly Balduzzi found that PISO had poor accuracy for torque coefficient while SIM-

PLE and Coupled were accurate, however Coupled allowed for the same performance at larger time steps than SIMPLE[135]. Daroczy showed that the Coupled solver produces identical results with 24 iterations per time step while PISO required 100 iterations[129].

Coupled should be the default option due to much faster convergence but if investigating wakes it's necessary to conduct a verification of both SIMPLE and Coupled.

4.1.5.4. Spatial Discretisation.

For the Spatial Discretisation, Almohammadi compared k-ε RNG and Transition SST using first and second order models[136]. They found a significant difference when using Transition SST with up to 1% change in C_p but a negligible difference for k-ε RNG, so individual verification is required.

4.1.5.5. Domain Size.

Rezaeiha[127][128][137] found that for 2D simulations a blockage ratio of 5%, or a domain width of 20D, is necessary for good prediction of C_p. Daroczy[129] supports this as although they stated that 50D was necessary, their results show that as low as 15D is sufficient. Balduzzi[135] however did find that a width of >40D was necessary, these changes can be visualised in figure 7. The reason for these differences is unclear as the magnitude of Reynolds number is similar for these studies, it may be due to Balduzzi's turbine design which wasn't published.

For inlet distance Rezaeiha found that 10D was adequate however 12.5D was a safer choice, but Balduzzi and Daroczy found that 20D was necessary. For outlet distance Rezaeiha showed that 10D is adequate for converged C_p prediction while 25D may be necessary if investigating wakes due to the asymmetrical outlet pressure experienced with smaller outlet distances. Balduzzi and Daroczy suggested higher requirements again with both suggesting >40D.

Rezaeiha demonstrated that the rotational domain diameter had a negligible effect. Dessoky showed that increasing TSR results in larger domain size requirements.

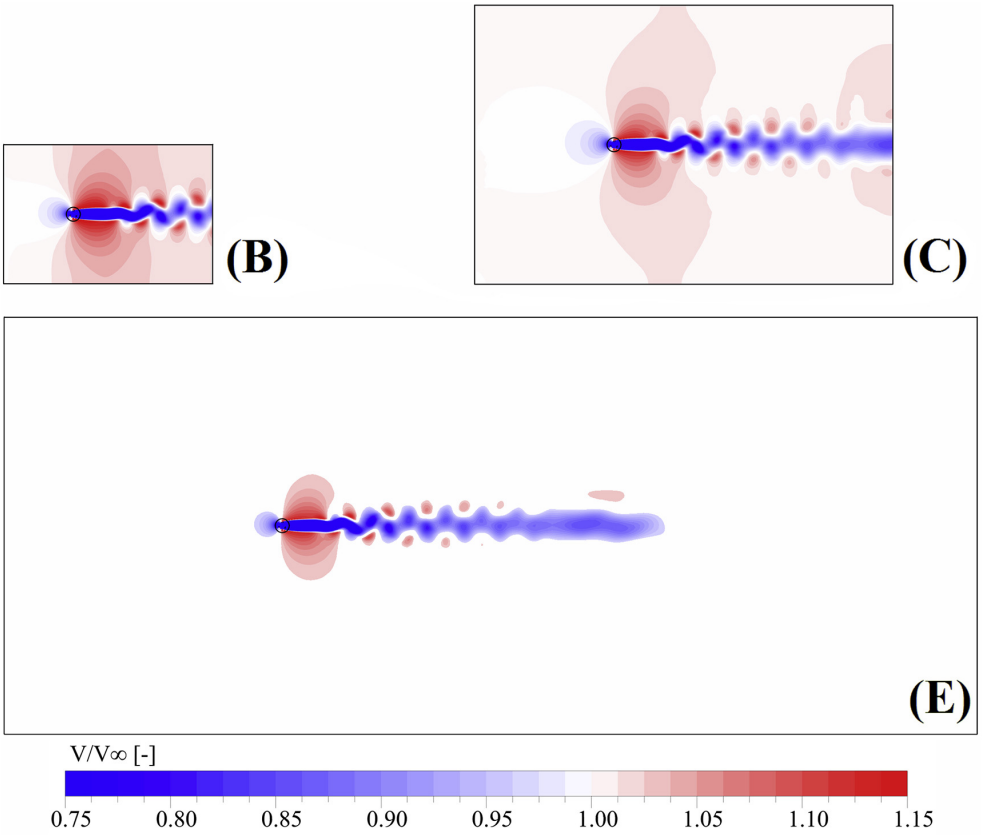

Figure 7: Velocity contours dependent on domain size [135]

Given the relatively few additional elements needed to increase domain size it is advisable to opt for a larger domain, giving an inlet length of 20D, outlet length of 40D, domain width of 40D or blockage ratio of 2.5%. Increasing the rotational domain size increases the element count considerably but has negligible effects, so a diameter of 1.25D is acceptable as demonstrated by Rezaeiha[127].

4.1.5.6. Time-step.

Significant variation between time step recommendations for both 2D and 3D is presented, with 2D being the most documented and most using rotational steps rather than time domain. Rezaeiha[137], Danao[130], and

Rosetti[105] all suggest that 0.5° increments are sufficient, with Rezaeiha and Danao clarifying it is only sufficient for high TSR>4.5 and 4 respectively, and the former finding that 1 degree is acceptable. Smaller increments must be used at lower TSR with Danao suggesting 0.25° and Rezaeiha 0.1°.

Balduzzi shows that the increment is dependent on the pressure-velocity coupling with Coupled allowing for larger steps than SIMPLE, recommending 0.9 and 0.27° respectively[135]. Balduzzi also finds that smaller time-steps are needed for coarser meshes, and that time-step size has a significant effect on blade wake prediction. Trivellato takes a Courant number oriented approach which is suited to free-spinning turbines by adapting time-steps to the variable rotational speed[138]. They find that CFL<0.15 is necessary for converged results, however it is recommended that this should be a maximum and smaller steps are ideal. Like Rezeaiha and Danao, Gosselin also demonstrated different increments for different TSRs, with 0.36° being adequate at high TSR and 0.072° necessary at lower TSR[10]. Based upon these studies it would be recommended for researchers to use time steps of 0.25° as a starting point and then verify themselves according to TSR used.

In 3D larger time steps are acceptable with Alaimo[5] showing near-convergence with 3.6° at TSR=0.89 and Elkhoury[35] showing convergence for both 1.2 and 0.6° at TSR=1, meaning the convergence point likely lies between 1.2 and 3.6°, even at low TSR. Further testing is necessary for verification.

4.1.5.7. Summary of Simulations.

Table 4: Recommended Settings for VAWT CFD

Turbulence Model	IDDES or k-ω SST
Pressure-Velocity Coupling	Coupled
2D or 3D Analysis	3D
Inlet Length	20D
Outlet Length	40D
Blockage Ratio	2.5%
Rotational Domain Diameter	1.25D
Rotational Step (2D)	0.25°
Rotational Step (3D)	1.2°

Several models are available for simulation with CFD offering the greatest accuracy. Non-CFD based models have good potential but require further development and most aren't usable for arrays. For most cases of conducting a CFD simulation, the settings described in table 1 should be used as a starting point.

4.2. Experimental Testing

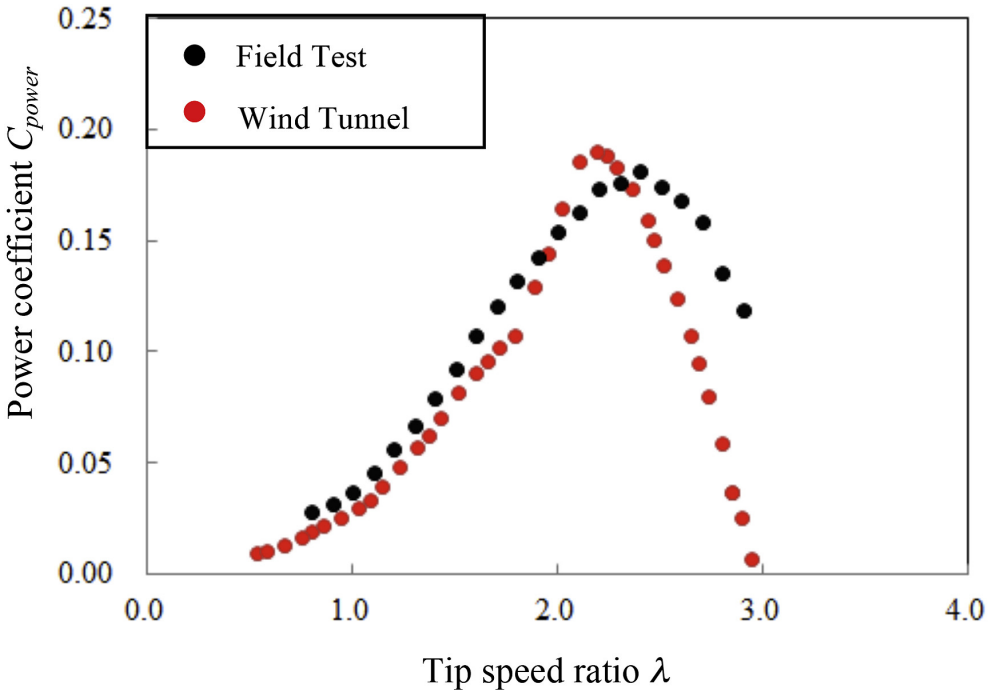

Figure 8: Comparison of TSR/ C_p curves for field and wind tunnel experiments [25]

Experimental testing typically uses a wind tunnel, however there are examples of field testing[25][139]. Li compared wind tunnel and field results with, as shown by figure 8, the wind tunnel TSR/C_p profile having a slightly higher $C_{p\text{-}max}$ and lower TSR_{opt} albeit with a smaller operating range[25]. Schito[140] also showed very different results between an Open-Jet wind tunnel and field testing for their VAWT in simulation. This shows that wind tunnel results may not be representative of real conditions which has major implications for evaluating the performance of new VAWT designs, and also

for evaluating simulation techniques. Sections 2.3.1 and 2.3.2 consider how to mitigate this.

Sun[141] conducts a review on measuring the wakes of turbines in the field, with many modern studies utilising Lidar. This method proves to be very cost effective compared to large wind tunnels, further supporting a preference for field experiments.

4.3. Wind Conditions

4.3.1. Boundary Conditions

Considerable variation in inlet velocities is seen amongst the literature, this is partly necessary as there is evidence that Reynolds number affects performance however there is little consistency in either, demonstrated by figures 9 and 10 which collate the distributions of inlet velocity and Reynolds number across studies referenced in this review.

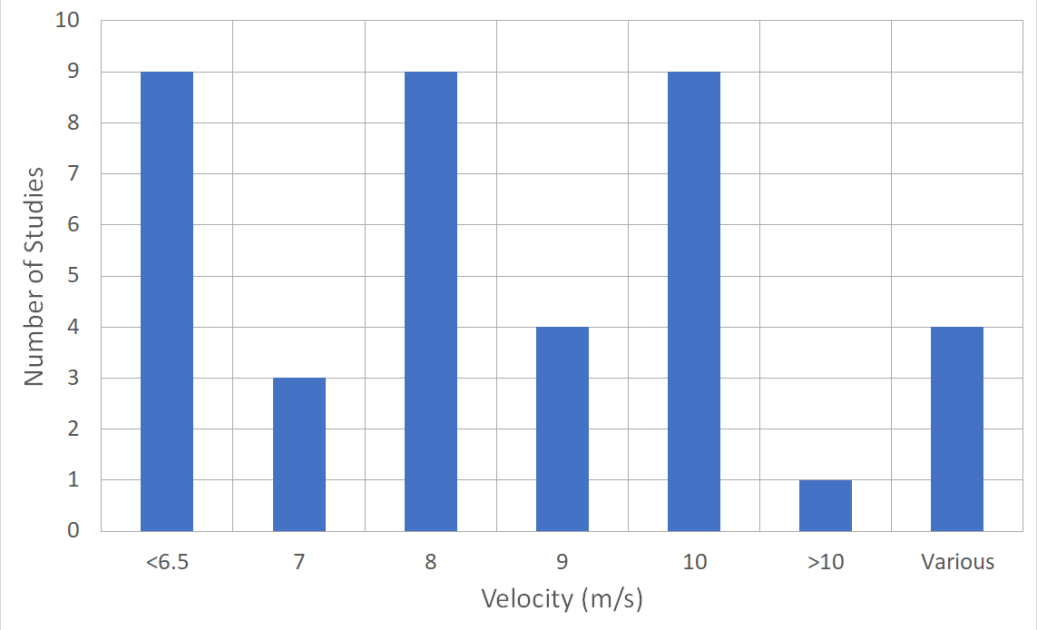

Figure 9: Distribution of Inlet Velocity by number of studies

Reynolds number is stated in two ways across studies, relating either to the chord of the blades or the diameter of the turbine. Bachant[27], using an experiment, shows chord Reynolds independence at $2.1 \text{x} 10^5$ with a

turbine Reynolds number of $0.8x10^6$. This is in line with Fiedler's experimental study[7] which found chord Reynolds independence at $2.1x10^5$ also. Rezaeiha[28] doesn't show chord Reynolds independence during their testing using 2D CFD. Blackwell's experimental results using a Φ-turbine shows that this is solidity dependent, with lower solidity turbines showing chord Reynolds independence at as low as $1.54x10^5$ while a turbine with a solidity of 0.3 didn't show independence at the highest tested value of $2.94x10^5$[12]. It should be noted that Bachant and Fiedler both used high solidity H-turbines of 0.48 and 0.4 respectively, while Blackwell used a Φ-turbine, which would affect results.

Rezaeiha's results may point to their CFD methodology failing to predict Reynolds independence, which would be an important insight into inaccuracy of some previous VAWT CFD modelling at certain ranges of Reynolds number, demonstrating a potential need for more detailed recreations of experiments in order to improve accuracy. This could include specifics such as surface roughness, boundary conditions, and using 3D CFD which are likely to affect Reynolds independence. Blackwell's results for their Φ turbine, in contrast to Bachant and Fiedler's H-bladed turbine results, suggest that different VAWT designs may have different points of Reynolds independence. This could be related to 3D effects which would explain the relationship between these results. It is necessary to demonstrate Reynolds independence in testing for results to be applicable to larger turbines. Bachant and Fiedler's results imply that Reynolds independence occurs in conditions expected at a scale above urban but below utility scale turbines. This poses challenges to researchers because there is low availability of wind tunnels which allow for adequate testing procedures at this scale and such testing is expensive, while field testing requires greater planning and makes controlling for boundary conditions difficult. However wind turbines at this scale are often used on farms, warehouses, and factories with many currently using solar panels for this purpose, so these offer markets for early commercial VAWTs at a scale which allows for Re independence.

4.3.2. Industrial Standards

The standard for commercial wind turbines is set by IEC64100 [142] and its amendments so manufacturers can prove that their product will perform adequately in the field. Here the wind conditions will be focused on, considering how or if a scenario has been tested in the literature to outline where

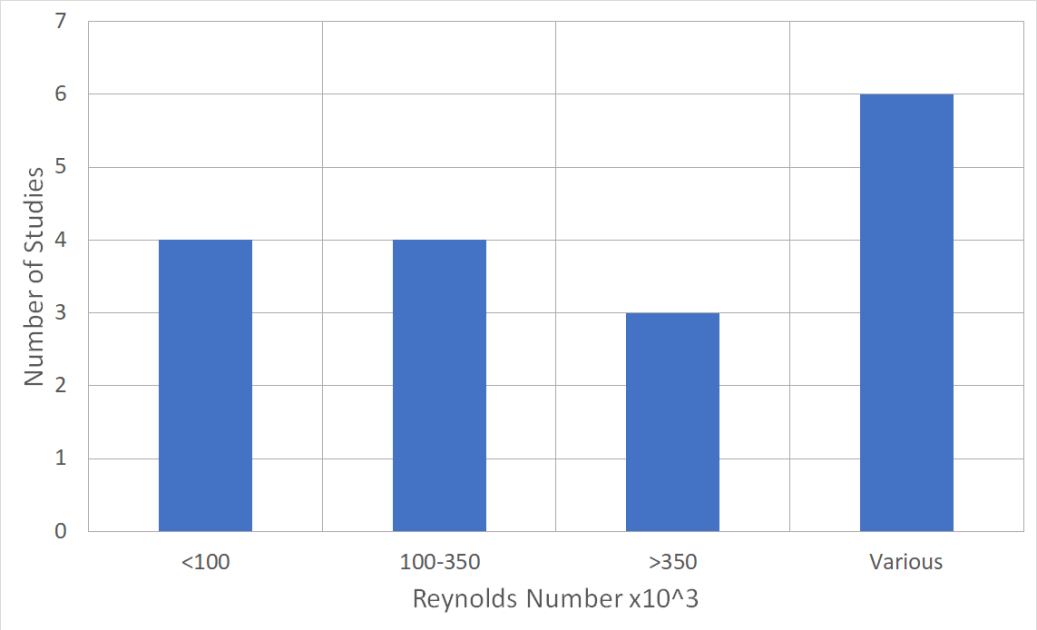

Figure 10: Distribution of Reynolds Number by number of studies

further research is necessary to better illustrate VAWT performance. All equations are sourced from IEC64100 [142].

4.3.2.1. Normal Wind Conditions.

Normal wind conditions are described by the following equations 6-8. Equation 6 denotes the distribution of wind speed based upon the class of turbine.

$$P_R = 1 - exp(-\pi(V_{hub}/2V_{avg})^2) \tag{6}$$

Where $V_{avg} = 0.2V_{ref}$ and V_{ref} is found from the wind turbine class I, II, or III. For a Class I turbine V_{ref} is 50m/s [142]. The normal distribution is used to calculate average power output by testing at different wind speeds to find the power curve of the turbine then using the distribution to find the average power output.

Equation 7 denotes the wind profile showing the boundary layer effect

$$V(z) = V(z_{ref})(z/z_{ref})^a \tag{7}$$

where a=0.2. The scenario described by equation 7 has been tested by Rolin[143] which uses boundary layer flow. Two pairs of counter-rotating vortices are produced by the VAWT and wake recovery is asymmetrical.

Equation 8 denotes the standard deviation of turbulence intensity.

$$\sigma_1 = I_{ref}(0.75V_{hub} + b) \tag{8}$$

where in equation 8, b=5.6m/s. σ_1, shall be given by the 90% quantile for the given hub height wind speed and I_{ref} is given by the class of turbine, where A=0.16, B=0.14, and C=0.12. For VAWTs V_{hub} should be considered as the velocity at the turbine mid-span.

While the turbulence profile isn't investigated directly, the effect of turbulence intensity is. Ahmadi-Baloutaki's experimental study finds that increasing turbulence intensity from <0.2% to 4-6% for an isolated turbine results in increased power output[85]. Bianchini finds that increasing turbulence intensity causes an increase in rotational speed, however this effect is insignificant between 0-10%[104]. However Untaroiu shows that decreasing turbulence intensity from 5% to 1% leads to a decrease in start-up time[144]. Li found that reducing turbulence intensity improves performance, however they used very high turbulence intensities with 25% being the lowest tested[25].

None of these studies used turbulence intensities aligned with the IEC64100 classes, so further research is necessary for the 12-16% region set out in classes A-C. This range should ideally be used in any VAWT research.

4.3.2.2. Extreme Wind Conditions.

Extreme wind conditions are described by the following equations and scenarios.

Equations 9 and 10 are the extreme wind speeds based upon likelihood of occurrence for 50 years and 1 year respectively.

$$V_{e50} = 1.4V_{ref}(z/z_{hub})^{0.11} \tag{9}$$

$$V_{e1} = 0.8V_{e50} \tag{10}$$

Equation 11 denotes longitudinal turbulence standard deviation.

$$\sigma_1 = 0.11V_{hub} \tag{11}$$

Equations 9-11 are variations upon what has been covered under normal wind conditions and can be tested by using higher wind speeds or Reynolds number.

Equation 12 denotes the maximum velocity of a gust, with equation 13 describing a scenario to test reaction to gusts.

$$V_{gust} = MIN\{ \begin{array}{c} 1.35(\mathrm{V}_{e1} - V_{hub}) \\ 3.3(\sigma_1/(1 + 0.1(D/\lambda_1)) \end{array} \tag{12}$$

where D is rotor diameter.

$$V(z,t) = \{ \begin{array}{cc} \mathrm{V(z)\text{-}0.37V}_{gust} sin(\frac{3\pi t}{T})(1 - cos(\frac{2\pi t}{T})) & 0<\mathrm{t}<\mathrm{T} \\ \mathrm{V(z)} & \text{otherwise} \end{array} \tag{13}$$

where V(z) is defined by the power law of equation 7 and T=10.5s. Scheurich[53] and Danao[130] both investigate unsteady wind speeds by using sinusoidal time-variant wind profiles, which while not the same as the scenario defined in equation 13, offer insight into VAWT behaviour under these conditions. Danao discovered that $\mathrm{TSR_{opt}}$ in unsteady conditions was slightly increased compared to steady conditions, and that ideally the fluctuations were small in amplitude ($<0.1\mathrm{V_{avg}}$) and high in frequency (>1Hz). Scheurich tested velocity fluctuations of 10% and 30%, finding that fluctuations of <10% can be treated as quasi-steady-state[53].

Equation 14 denotes the standard deviation of extreme turbulence.

$$\sigma_1 = cI_{ref}(0.072((\frac{V_{avg}}{c}) + 3)(\frac{V_{hub}}{c} - 4) + 10) \tag{14}$$

where c=2m/s

Equations 15 and 16 describe the scenario of an extreme direction change

$$\theta_e = \pm 4tan^{-1}(\sigma_1/(V_{hub}(1 + 0.1(D/\lambda_1)))) \tag{15}$$

$$\theta(t) = \{ \begin{array}{cc} 0 & \mathrm{t}<0 \\ \pm 0.5\theta_e(1 - cos(\frac{\pi t}{T})) & 0<\mathrm{t}<\mathrm{T} \\ \theta_e & \mathrm{t}>\mathrm{T}. \end{array} \tag{16}$$

where T=6s is the duration of the extreme direction change. ϑ_e denotes the direction change magnitude while $\vartheta(\mathrm{t})$ represents the transient process of the direction change.

Similarly vertically skewed flow should be considered, although this isn't included in IEC64100. Chowdhury found that tilted turbines show a significant increase in $\mathrm{C_p}$ at high tilts[84], but worse wake recovery. This is likely due to the higher swept area and reduced effects of leading blade wakes.

Equations 17-20 describe the scenario of an extreme coherent gust with a direction change.

$$V(z,t) = \{ \begin{array}{cc} \text{V(z)} & \text{t<0} \\ \text{V(z)+0.5V}_{cg}(1 - cos(\frac{\pi t}{T}) & \text{0<t<T} \\ \text{V(z)+V}_{cg} & \text{t>T} \end{array} \quad (17)$$

$$V_{cg} = 15m/s \quad (18)$$

where T=10s

$$\theta_{\text{cg}} = \{ \begin{array}{cc} \text{180 degrees} & \text{V}_{\text{hub}}\text{<4m/s} \\ \text{(720 degrees m/s) /V}_{hub} & \text{4m/s <V}_{hub}\text{<}V_{ref} \end{array} \quad (19)$$

$$\theta(t) = \{ \begin{array}{cc} \text{0 degrees} & \text{t<0} \\ \pm 0.5\theta_{cg}(1 - cos(\frac{\pi t}{T})) & \text{0<t<T} \\ \pm\theta_{cg} & \text{t} \end{array} \quad (20)$$

where T=10s

While researchers may consider that this scenario is unlikely to have any significant effect on VAWTs given their inherent omnidirectionality, Wu[145] found otherwise, with lateral gusts causing significant changes in power output. The magnitude and direction of the change depended on aerofoil, TSR, gust magnitude, and number of blades. Reductions in performance were found at TSR=3 while small increases were seen at TSR=4, which is important as this is the common range for VAWTs. Further analysis is needed in this region in order to consider the transition through no performance impact. Symmetrical aerofoils had similar relationships between C_p change and TSR with small increases from TSR 4 to 7. At TSR=3, the NACA0018 aerofoil had a markedly smaller reduction in performance than the other symmetrical aerofoils (-2.92% compared to -8.92% and -11.43%). The tested cambered aerofoil had power decreases of up to 17% at higher TSR, which could risk poor off-design performance.

$$V(z,t) = \{ \begin{array}{cc} \text{V}_{hub}((\frac{z}{z_{hub}})^a) \pm (\frac{z-z_{hub}}{D})(2.5 + 0.2\beta\sigma_1(\frac{D}{\lambda_1})^{\frac{1}{4}})(1 - cos(\frac{2\pi t}{T})) & \text{0 <t} \\ \text{V}_{hub}(\frac{z}{z_{hub}})^a & \text{otherwise} \end{array} \quad (21)$$

$$V(y,z,t) = \{ \begin{array}{cc} \mathrm{V}_{hub}((\frac{z}{z_{hub}})^a \pm \frac{y}{D}(2.5 + 0.2\beta\sigma_1(\frac{D}{\lambda_1})^{\frac{1}{4}})(1 - \frac{cos(2\pi t}{T})) & 0<\mathrm{t}<\mathrm{T} \\ \mathrm{V}_{hub}(\frac{z}{z_{hub}})^a & \text{otherwise} \end{array} \quad (22)$$

where a=0.2, β=6.4, T=12s.

The sign for the horizontal wind shear transient shall be chosen so that the worst transient loading occurs rather than both extreme shears being applied simultaneously.

Equations 21 and 22 consider the extreme wind shear in horizontal and vertical directions respectively. Regarding VAWTs the vertical shear can affect performance due to the change in velocity along the blade, this is notable for helical VAWTs as it impacts their torque ripple. Horizontal shear may affect performance as it changes the effective freestream velocity depending on the position of the blade.

4.3.3. Summary of Experimental Design

Field testing should be used when possible. Future research should assess Reynolds dependence during experimental design. The vastness of the IEC64100 specification makes it difficult to analyse a new design against all requirements.

5. Conclusion

The testing and development of VAWTs remains a challenge but it has become more viable. 3D simulations provide clear advantages, and under the proposed guidelines which allow for much larger time steps and a relatively coarse mesh compared to 2D, authors may find a smaller time penalty than previously expected. Another mainstream viewpoint has been challenged in that the current equation for solidity in equation 2 is a poor measure and should be separated into chord length and blade density in order to improve comparability between turbines. Field testing may be a better experimental option than wind tunnels due to the clear differences in the TSR/C_p curve reducing applicability of wind tunnel results. Further consideration must be given to higher level turbine design alongside farm design, particularly if wishing to commercialise a turbine.

Acknowledgement

Funding: This work was supported by an EPSRC Doctoral Training Scholarship (Grant No. 2119005).

References

[1] Robert E Akins, Dale E Berg, and W Tait Cyrus. SANDIA REPORT Measurements and Calculations of Aerodynamic Torques for a Vertical-Axis Wind Turbine. Technical report, 1987. URL `https://energy.sandia.gov/wp-content/gallery/uploads/SAND-86-2164.pdf`. Accessed on 22.05.2019.

[2] Gabriele Bedon, Uwe Schmidt Paulsen, Helge Aagaard Madsen, Federico Belloni, Marco Raciti Castelli, and Ernesto Benini. Computational assessment of the DeepWind aerodynamic performance with different blade and airfoil configurations. *Applied Energy*, 185:1100–1108, jan 2017. ISSN 03062619. doi: 10.1016/j.apenergy.2015.10.038.

[3] Albert Betz and D. G. Randall. *Introduction to the theory of flow machines*. 1966. ISBN 9781483180908.

[4] Amgad Dessoky, Thorsten Lutz, Galih Bangga, and Ewald Krämer. Computational studies on Darrieus VAWT noise mechanisms employing a high order DDES model. *Renewable Energy*, 143:404–425, dec 2019. ISSN 0960-1481. doi: 10.1016/J.RENENE.2019.04.133. URL `https://www.sciencedirect.com/science/article/pii/S0960148119306160{\#}fig5`.

[5] Andrea Alaimo, Antonio Esposito, Antonio Messineo, Calogero Orlando, and Davide Tumino. 3D CFD analysis of a vertical axis wind turbine. *Energies*, 8(4):3013–3033, 2015. ISSN 19961073. doi: 10.3390/en8043013.

[6] Changping Liang, Deke Xi, Sen Zhang, and Qiuping Yang. IOP Conference Series: Earth and Environmental Science Effects of Solidity on Aerodynamic Performance of H-Type Vertical Axis Wind Turbine Effects of Solidity on Aerodynamic Performance of H-Type Vertical Axis Wind Turbine. *IOP Conf. Ser.: Earth Environ. Sci*, 170:42061, 2018. doi: 10.1088/1755-1315/170/4/042061. URL `https://iopscience.iop.org/article/10.1088/1755-1315/170/4/042061/pdf`.

[7] Andrzej J Fiedler and Stephen Tullis. Blade Offset and Pitch Effects on a High Solidity Vertical Axis Wind Turbine. Technical report, 2009. URL https://journals.sagepub.com/doi/pdf/10.1260/030952409789140955.

[8] A. Sagharichi, M. Zamani, and A. Ghasemi. Effect of solidity on the performance of variable-pitch vertical axis wind turbine. *Energy*, 161: 753–775, oct 2018. ISSN 0360-5442. doi: 10.1016/J.ENERGY.2018.07.160. URL https://www.sciencedirect.com/science/article/pii/S0360544218314579?via{\%}3Dihub.

[9] Brian Hand and Andrew Cashman. Conceptual design of a large-scale floating offshore vertical axis wind turbine. *Energy Procedia*, 142: 83–88, dec 2017. ISSN 1876-6102. doi: 10.1016/J.EGYPRO.2017.12.014. URL https://www.sciencedirect.com/science/article/pii/S1876610217357417.

[10] Remi Gosselin. *Analysis and optimization of vertical axis turbines*. PhD thesis, Université Laval, 2015.

[11] Abdolrahim Rezaeiha, Hamid Montazeri, and Bert Blocken. Towards optimal aerodynamic design of vertical axis wind turbines: Impact of solidity and number of blades. *Energy*, 165:1129–1148, dec 2018. ISSN 0360-5442. doi: 10.1016/J.ENERGY.2018.09.192. URL https://www.sciencedirect.com/science/article/pii/S0360544218319704.

[12] B F Blackwell, R E Sheldahl, and L V Feltz. Wind tunnel performance data for the Darrieus wind turbine with NACA 0012 blades. (May), 1976. doi: 10.2172/7269797. URL http://www.osti.gov/servlets/purl/7269797/.

[13] Robert Howell, Ning Qin, Jonathan Edwards, and Naveed Durrani. Wind tunnel and numerical study of a small vertical axis wind turbine. *Renewable Energy*, 35(2):412–422, feb 2010. ISSN 0960-1481. doi: 10.1016/J.RENENE.2009.07.025. URL https://www.sciencedirect.com/science/article/pii/S0960148109003048.

[14] Palash Jain and A. Abhishek. Performance prediction and fundamental understanding of small scale vertical axis wind turbine

with variable amplitude blade pitching. *Renewable Energy*, 97:97–113, nov 2016. ISSN 0960-1481. doi: 10.1016/J.RENENE.2016.05.056. URL https://www.sciencedirect.com/science/article/pii/S0960148116304669.

[15] Young-Tae Lee and Hee-Chang Lim. Numerical study of the aerodynamic performance of a 500 W Darrieus-type vertical-axis wind turbine. *Renewable Energy*, 83:407–415, nov 2015. ISSN 0960-1481. doi: 10.1016/J.RENENE.2015.04.043. URL https://www.sciencedirect.com/science/article/pii/S0960148115003237.

[16] M.H. Mohamed. Impacts of solidity and hybrid system in small wind turbines performance. *Energy*, 57:495–504, aug 2013. ISSN 0360-5442. doi: 10.1016/J.ENERGY.2013.06.004. URL https://www.sciencedirect.com/science/article/pii/S0360544213005021.

[17] M C Claessens. *The Design and Testing of Airfoils for Application in Small Vertical Axis Wind Turbines*. PhD thesis, TU Delft, 2006. URL http://lr.home.tudelft.nl/fileadmin/Faculteit/LR/Organisatie/Afdelingen{_}en{_}Leerstoelen/Afdeling{_}AEWE/Aerodynamics/Contributor{_}Area/Secretary/M.{_}Sc.{_}theses/doc/2006{_}1{_}17.pdf.

[18] Delphine De Tavernier, Carlos Ferreira, and Gerard Bussel. Airfoil optimisation for vertical-axis wind turbines with variable pitch. *Wind Energy*, 22(4):547–562, apr 2019. ISSN 1095-4244. doi: 10.1002/we.2306. URL https://onlinelibrary.wiley.com/doi/abs/10.1002/we.2306.

[19] L. Battisti, A. Brighenti, E. Benini, and M. Raciti Castelli. Analysis of Different Blade Architectures on small VAWT Performance. *Journal of Physics: Conference Series*, 753:062009, sep 2016. ISSN 1742-6588. doi: 10.1088/1742-6596/753/6/062009. URL http://stacks.iop.org/1742-6596/753/i=6/a=062009?key=crossref.7e5591e63e014af59f1600ce504c474d.

[20] Herbert J Sutherland, Dale E Berg, and Thomas D Ashwill. SANDIA REPORT A Retrospective of VAWT Technology. Technical report, 2012. URL https://energy.sandia.gov/wp-content/gallery/uploads/SAND2012-0304.pdf. Accessed on 22.05.2019.

[21] R. E. Sheldahl, P. Klimas, and L. Feltz. Aerodynamic Performance of a 5-Metre- Diameter Darrieus Turbine With Extruded Aluminum NACA-0015 Blades. *Sandia Laboratories*, 1980.

[22] S. Brusca, R. Lanzafame, and M. Messina. Design of a vertical-axis wind turbine: how the aspect ratio affects the turbine's performance. *International Journal of Energy and Environmental Engineering*, 5(4): 333–340, dec 2014. ISSN 2008-9163. doi: 10.1007/s40095-014-0129-x. URL `http://link.springer.com/10.1007/s40095-014-0129-x`.

[23] Stefania Zanforlin and Stefano Deluca. Effects of the Reynolds number and the tip losses on the optimal aspect ratio of straight-bladed Vertical Axis Wind Turbines. *Energy*, 148:179–195, apr 2018. ISSN 0360-5442. doi: 10.1016/J.ENERGY.2018.01.132. URL `https://www.sciencedirect.com/science/article/pii/S0360544218301609`.

[24] Sung-Cheoul Roh and Kang Seung-Hee. Effects of a blade profile, the Reynolds number, and the solidity on the performance of a straight bladed vertical axis wind turbine. *Journal of Mechanical Science and Technology*, 27(11):3299–3307, 2013. doi: 10.1007/s12206-013-0852-x. URL `www.springerlink.com/content/1738-494x`.

[25] Qing'an Li, Takao Maeda, Yasunari Kamada, Junsuke Murata, Masayuki Yamamoto, Tatsuhiko Ogasawara, Kento Shimizu, and Tetsuya Kogaki. Study on power performance for straight-bladed vertical axis wind turbine by field and wind tunnel test. *Renewable Energy*, 90:291–300, may 2016. ISSN 09601481. doi: 10.1016/j.renene.2016.01.002. URL `https://linkinghub.elsevier.com/retrieve/pii/S0960148116300027`.

[26] K. McLaren, S. Tullis, and S. Ziada. Computational fluid dynamics simulation of the aerodynamics of a high solidity, small-scale vertical axis wind turbine. *Wind Energy*, 15(3):349–361, apr 2012. ISSN 10954244. doi: 10.1002/we.472. URL `http://doi.wiley.com/10.1002/we.472`.

[27] Peter Bachant, Martin Wosnik, Peter Bachant, and Martin Wosnik. Effects of Reynolds Number on the Energy Conversion and Near-Wake

Dynamics of a High Solidity Vertical-Axis Cross-Flow Turbine. *Energies*, 9(2):73, jan 2016. ISSN 1996-1073. doi: 10.3390/en9020073. URL http://www.mdpi.com/1996-1073/9/2/73.

[28] Abdolrahim Rezaeiha, Hamid Montazeri, and Bert Blocken. Characterization of aerodynamic performance of vertical axis wind turbines: Impact of operational parameters. *Energy Conversion and Management*, 169:45–77, aug 2018. ISSN 0196-8904. doi: 10.1016/J.ENCONMAN.2018.05.042. URL https://www.sciencedirect.com/science/article/pii/S0196890418305193?via{\%}3Dihub.

[29] H.Y. Peng, H.F. Lam, and H.J. Liu. Power performance assessment of H-rotor vertical axis wind turbines with different aspect ratios in turbulent flows via experiments. *Energy*, 173:121–132, apr 2019. ISSN 0360-5442. doi: 10.1016/J.ENERGY.2019.01.140. URL https://www.sciencedirect.com/science/article/pii/S0360544219301562?via{\%}3Dihub{\#}!

[30] Seyed Hossein Hezaveh, Elie Bou-Zeid, Mark W. Lohry, and Luigi Martinelli. Simulation and wake analysis of a single vertical axis wind turbine. *Wind Energy*, 20(4):713–730, apr 2017. ISSN 10954244. doi: 10.1002/we.2056. URL http://doi.wiley.com/10.1002/we.2056.

[31] Mahdi Torabi Asr, Erfan Zal Nezhad, Faizal Mustapha, and Surjatin Wiriadidjaja. Study on start-up characteristics of H-Darrieus vertical axis wind turbines comprising NACA 4-digit series blade airfoils. *Energy*, 112:528–537, oct 2016. ISSN 0360-5442. doi: 10.1016/J.ENERGY.2016.06.059. URL https://www.sciencedirect.com/science/article/pii/S0360544216308337?via{\%}3Dihub{\#}bib21.

[32] Louis Angelo Danao, Ning Qin, and Robert Howell. A numerical study of blade thickness and camber effects on vertical axis wind turbines. *Proceedings of the Institution of Mechanical Engineers, Part A: Journal of Power and Energy*, 226(7):867–881, nov 2012. ISSN 0957-6509. doi: 10.1177/0957650912454403. URL http://journals.sagepub.com/doi/10.1177/0957650912454403.

[33] Mazharul Islam, David S-K. Ting, and Amir Fartaj. Design of a Special-Purpose Airfoil for Smaller-Capacity Straight-Bladed VAWT.

Wind Engineering, 31(6):401–424, dec 2007. ISSN 0309-524X. doi: 10.1260/030952407784079780. URL http://journals.sagepub.com/doi/10.1260/030952407784079780.

[34] Carlos Simão Ferreira. *The near wake of the VAWT 2D and 3D views of the VAWT aerodynamics The near wake of the VAWT*. PhD thesis, TU Delft, 2009. URL https://www.researchgate.net/profile/Carlos{_}Ferreira17/publication/27353842{_}The{_}near{_}wake{_}of{_}the{_}VAWT{_}2d{_}and{_}3d{_}views{_}of{_}the{_}VAWT{_}aerodynamics/links/00b7d534b8fb84e807000000.pdf.

[35] M. Elkhoury, T. Kiwata, and E. Aoun. Experimental and numerical investigation of a three-dimensional vertical-axis wind turbine with variable-pitch. *Journal of Wind Engineering and Industrial Aerodynamics*, 139:111–123, apr 2015. ISSN 0167-6105. doi: 10.1016/J.JWEIA.2015.01.004. URL https://www.sciencedirect.com/science/article/pii/S0167610515000136{\#}bib16.

[36] Gabriele Bedon, Stefano De Betta, and Ernesto Benini. Performance-optimized airfoil for Darrieus wind turbines. *Renewable Energy*, 94:328–340, aug 2016. ISSN 0960-1481. doi: 10.1016/J.RENENE.2016.03.071. URL https://www.sciencedirect.com/science/article/pii/S0960148116302555{\#}bib15.

[37] Jian Chen, Liu Chen, Hongtao Xu, Hongxing Yang, Changwen Ye, and Di Liu. Performance improvement of a vertical axis wind turbine by comprehensive assessment of an airfoil family. *Energy*, 114:318–331, nov 2016. ISSN 0360-5442. doi: 10.1016/J.ENERGY.2016.08.005. URL https://www.sciencedirect.com/science/article/pii/S0360544216311082.

[38] Jabir Ubaid Parakkal, Khadije El Kadi, Ameen El-Sinawi, Sherine Elagroudy, and Isam Janajreh. Numerical analysis of VAWT wind turbines: Joukowski vs classical NACA rotor's blades. *Energy Procedia*, 158:1194–1201, feb 2019. ISSN 18766102. doi: 10.1016/j.egypro.2019.01.306. URL https://linkinghub.elsevier.com/retrieve/pii/S1876610219303261.

[39] M.H. Mohamed, A.M. Ali, and A.A. Hafiz. CFD analysis for H-rotor Darrieus turbine as a low speed wind energy converter. *Engineering Science and Technology, an International Journal*, 18(1): 1–13, mar 2015. ISSN 2215-0986. doi: 10.1016/J.JESTCH.2014.08.002. URL https://www.sciencedirect.com/science/article/pii/S2215098614000585{\#}bib4.

[40] M.H. Mohamed. Performance investigation of H-rotor Darrieus turbine with new airfoil shapes. *Energy*, 47(1):522–530, nov 2012. ISSN 0360-5442. doi: 10.1016/J.ENERGY.2012.08.044. URL https://www.sciencedirect.com/science/article/pii/S0360544212006755.

[41] Francesco Balduzzi, Alessandro Bianchini, Riccardo Maleci, Giovanni Ferrara, and Lorenzo Ferrari. Blade Design Criteria to Compensate the Flow Curvature Effects in H-Darrieus Wind Turbines. *Journal of Turbomachinery*, 137(1):011006, sep 2014. ISSN 0889-504X. doi: 10.1115/1.4028245. URL http://turbomachinery.asmedigitalcollection.asme.org/article.aspx?doi=10.1115/1.4028245.

[42] Alessandro Bianchini, Francesco Balduzzi, Giovanni Ferrara, and Lorenzo Ferrari. Virtual incidence effect on rotating airfoils in Darrieus wind turbines. *Energy Conversion and Management*, 111:329–338, mar 2016. ISSN 0196-8904. doi: 10.1016/j.enconman.2015.12.056. URL https://www.sciencedirect.com/science/article/pii/S0196890415011656.

[43] Ning Ma, Hang Lei, Zhaolong Han, Dai Zhou, Yan Bao, Kai Zhang, Lei Zhou, and Caiyong Chen. Airfoil optimization to improve power performance of a high-solidity vertical axis wind turbine at a moderate tip speed ratio. *Energy*, 150:236–252, may 2018. ISSN 0360-5442. doi: 10.1016/J.ENERGY.2018.02.115. URL https://www.sciencedirect.com/science/article/pii/S0360544218303499.

[44] Travis J. Carrigan, Brian H. Dennis, Zhen X. Han, and Bo P. Wang. Aerodynamic Shape Optimization of a Vertical-Axis Wind Turbine Using Differential Evolution. *ISRN Renewable Energy*, 2012:1–16, 2012. ISSN 2090-746X. doi: 10.5402/2012/528418. URL https://www.hindawi.com/archive/2012/528418/.

[45] Carlos Simão Ferreira and Ben Geurts. Aerofoil optimization for vertical-axis wind turbines. *Wind Energy*, 18(8):1371–1385, aug 2015. ISSN 10954244. doi: 10.1002/we.1762. URL http://doi.wiley.com/10.1002/we.1762.

[46] M. Jafaryar, R. Kamrani, M. Gorji-Bandpy, M. Hatami, and D.D. Ganji. Numerical optimization of the asymmetric blades mounted on a vertical axis cross-flow wind turbine. *International Communications in Heat and Mass Transfer*, 70:93–104, jan 2016. ISSN 0735-1933. doi: 10.1016/J.ICHEATMASSTRANSFER.2015.12.003. URL https://www.sciencedirect.com/science/article/pii/S0735193315002511.

[47] Shawn Armstrong, Andrzej Fiedler, and Stephen Tullis. Flow separation on a high Reynolds number, high solidity vertical axis wind turbine with straight and canted blades and canted blades with fences. *Renewable Energy*, 41:13–22, may 2012. ISSN 0960-1481. doi: 10.1016/J.RENENE.2011.09.002. URL https://www.sciencedirect.com/science/article/pii/S0960148111005209{\#}bib1.

[48] Abdolrahim Rezaeiha, Ivo Kalkman, and Bert Blocken. Effect of pitch angle on power performance and aerodynamics of a vertical axis wind turbine. *Applied Energy*, 197:132–150, jul 2017. ISSN 0306-2619. doi: 10.1016/J.APENERGY.2017.03.128. URL https://www.sciencedirect.com/science/article/pii/S0306261917303744?via{\%}3Dihub{\#}b0135.

[49] Ion Paraschivoiu, Octavian Trifu, and F. Saeed. H-Darrieus wind turbine with blade pitch control. *International Journal of Rotating Machinery*, 2009, 2009. ISSN 1023621X. doi: 10.1155/2009/505343.

[50] Gebreel Abdalrahman, William Melek, and Fue-Sang Lien. Pitch angle control for a small-scale Darrieus vertical axis wind turbine with straight blades (H-Type VAWT). *Renewable Energy*, 114:1353–1362, dec 2017. ISSN 0960-1481. doi: 10.1016/J.RENENE.2017.07.068. URL https://www.sciencedirect.com/science/article/pii/S0960148117306961.

[51] PL Delafin, T Nishino, L Wang, and A Kolios. Effect of the number of blades and solidity on the performance of a vertical axis wind turbine Related content Effects of Solidity on Aerodynamic

Performance of H-Type Vertical Axis Wind Turbine. *Journal of physics: Conference Series*, 753, 2016. doi: 10.1088/1742-6596/753/2/022033. URL http://iopscience.iop.org/article/10.1088/1742-6596/753/2/022033/pdf.

[52] Wendi Liu and Qing Xiao. Investigation on Darrieus type straight blade vertical axis wind turbine with flexible blade. *Ocean Engineering*, 110: 339–356, 2015. ISSN 00298018. doi: 10.1016/j.oceaneng.2015.10.027. URL http://dx.doi.org/10.1016/j.oceaneng.2015.10.027.

[53] Frank Scheurich and Richard E. Brown. Modelling the aerodynamics of vertical-axis wind turbines in unsteady wind conditions. *Wind Energy*, 16(1):91–107, jan 2013. ISSN 10954244. doi: 10.1002/we.532. URL http://doi.wiley.com/10.1002/we.532.

[54] Mahamed Hussain, Mostafa Sahed, Agnimitra Mazarbhuiya, Kaushal Biswas, and Sharma Kumar. Performance investigations of modified asymmetric blade H-Darrieus VAWT rotors. *J. Renewable Sustainable Energy*, 10:33302, 2018. doi: 10.1063/1.5026857. URL https://doi.org/10.1063/1.5026857.

[55] V. Samsonov and P. Baklushin. Comparison of different ways for VAWT aerodynamic control. *Journal of Wind Engineering and Industrial Aerodynamics*, 39(1-3):427–433, jan 1992. ISSN 0167-6105. doi: 10.1016/0167-6105(92)90566-S. URL https://www.sciencedirect.com/science/article/pii/016761059290566S.

[56] Yan Yan, Eldad Avital, and John Williams. CFD Analysis for the Performance of Gurney Flap on Aerofoil and Vertical Axis Turbine. 2019. doi: 10.18178/ijmerr.8.3.385-392. URL http://www.ijmerr.com/uploadfile/2019/0418/20190418104445638.pdf.

[57] Ion Malael, Radu Bogateanu, Horia Dumitrescu, and Corresponding Author. Theoretical performances of double Gurney Flap equipped the VAWTs. *INCAS BULLETIN*, 4:93–99, 2012. doi: 10.13111/2066-8201.2012.4.4.8. URL https://core.ac.uk/download/pdf/26891176.pdf.

[58] Haitian Zhu, Wenxing Hao, Chun Li, and Qinwei Ding. Numerical study of effect of solidity on vertical axis wind turbine with Gurney flap. *Journal of Wind Engineering and Industrial Aerodynamics*,

186:17–31, mar 2019. ISSN 0167-6105. doi: 10.1016/J.JWEIA.2018.12.016. URL https://www.sciencedirect.com/science/article/pii/S016761051830638X.

[59] Junwei Zhong, Jingyin Li, and Penghua Guo. Effects of leading-edge rod on dynamic stall performance of a wind turbine airfoil. *Journal of Power and Energy*, 231(8):753–769, 2017. doi: 10.1177/0957650917718453.

[60] Yichen Jiang, Chenlu He, Peidong Zhao, and Tiezhi Sun. Investigation of Blade Tip Shape for Improving VAWT Performance. *Journal of Marine Science and Engineering*, 8(225), 2020.

[61] Thierry Villeneuve, Matthieu Boudreau, and Guy Dumas. Improving the efficiency and the wake recovery rate of vertical-axis turbines using detached end-plates. *Renewable Energy*, 150:31–45, may 2020. ISSN 09601481. doi: 10.1016/j.renene.2019.12.088.

[62] Santiago Laín, Manuel Taborda, and Omar López. Numerical Study of the Effect of Winglets on the Performance of a Straight Blade Darrieus Water Turbine. *Energies*, 11(2):297, jan 2018. ISSN 1996-1073. doi: 10.3390/en11020297. URL http://www.mdpi.com/1996-1073/11/2/297.

[63] Tian-tian Zhang, Mohamed Elsakka, Wei Huang, Zhen-guo Wang, Derek B. Ingham, Lin Ma, and Mohamed Pourkashanian. Winglet design for vertical axis wind turbines based on a design of experiment and CFD approach. *Energy Conversion and Management*, 195:712–726, sep 2019. ISSN 0196-8904. doi: 10.1016/J.ENCONMAN.2019.05.055. URL https://www.sciencedirect.com/science/article/pii/S0196890419306107?via{\%}3Dihub.

[64] Binyamin Sasson and David Greenblatt. Effect of Leading-Edge Slot Blowing on a Vertical Axis Wind Turbine. *AIAA Journal*, 49(9):1932–1942, sep 2011. ISSN 0001-1452. doi: 10.2514/1.J050851. URL https://arc.aiaa.org/doi/10.2514/1.J050851.

[65] Abdolrahim Rezaeiha, Hamid Montazeri, and Bert Blocken. Active flow control for power enhancement of vertical axis wind turbines: Leading-edge slot suction. *Energy*, 189:116131, dec 2019. ISSN 03605442. doi: 10.1016/j.energy.2019.116131.

[66] Haitian Zhu, Wenxing Hao, Chun Li, and Qinwei Ding. Simulation on flow control strategy of synthetic jet in an vertical axis wind turbine. *Aerospace Science and Technology*, 77: 439–448, jun 2018. ISSN 1270-9638. doi: 10.1016/J.AST.2018.03.012. URL https://www.sciencedirect.com/science/article/pii/S1270963817317005{\#}br0060.

[67] Omar S. Mohamed, Ahmed A. Ibrahim, Ahmed K. Etman, Amr A. Abdelfatah, and Ahmed M.R. Elbaz. Numerical investigation of Darrieus wind turbine with slotted airfoil blades. *Energy Conversion and Management: X*, 5:100026, jan 2020. ISSN 25901745. doi: 10.1016/j.ecmx.2019.100026.

[68] Ning Qin, Robert Howell, Naveed Durrani, Kenichi Hamada, and Tomos Smith. Unsteady Flow Simulation and Dynamic Stall Behaviour of Vertical Axis Wind Turbine Blades. *Wind Engineering*, 35(4):511–527, aug 2011. ISSN 0309-524X. doi: 10.1260/0309-524X.35.4.511. URL http://journals.sagepub.com/doi/10.1260/0309-524X.35.4.511.

[69] Anders Goude, Staffan Lundin, and Mats Leijon. A parameter study of the influence of struts on the performance of a vertical-axis marine current turbine. In *8th European Wave and Tidal Energy Conference*, pages 477–482, Uppsala, Sweden, 2009. URL http://www.homepages.ed.ac.uk/shs/WaveEnergy/EWTEC2009/EWTEC2009(D)/papers/252.pdf.

[70] Victor Mendoza. Aerodynamic Studies of Vertical Axis Wind Turbines using the Actuator Line Model. Digital Comprehensive Summaries of Uppsala Dissertations from the Faculty of Science and Technology 1671. volume 85, 2018. ISBN 978-91-513-0338-3. URL http://urn.kb.se/resolve?urn=urn:nbn:se:uu:diva-348346.

[71] Zhenyu Wang and Mei Zhuang. Leading-edge serrations for performance improvement on a vertical-axis wind turbine at low tip-speed-ratios. *Applied Energy*, 208:1184–1197, dec 2017. ISSN 0306-2619. doi: 10.1016/J.APENERGY.2017.09.034. URL https://www.sciencedirect.com/science/article/pii/S0306261917313181?via{\%}3Dihub.

[72] Mahdi Zamani, Saeed Nazari, Sajad A. Moshizi, and Mohammad Javad Maghrebi. Three dimensional simulation of J-shaped Darrieus vertical axis wind turbine. *Energy*, 116(December):1243–1255, 2016. ISSN 03605442. doi: 10.1016/j.energy.2016.10.031. URL http://dx.doi.org/10.1016/j.energy.2016.10.031.

[73] Mahdi Zamani, Mohammad Javad Maghrebi, and Seyed Rasoul Varedi. Starting torque improvement using J-shaped straight-bladed Darrieus vertical axis wind turbine by means of numerical simulation. *Renewable Energy*, 95:109–126, sep 2016. ISSN 0960-1481. doi: 10.1016/J.RENENE.2016.03.069. URL https://www.sciencedirect.com/science/article/pii/S0960148116302531?via{\%}3Dihub{\#}fig4.

[74] Lin Pan, Haodong Xiao, Yanwei Zhang, and Zhaoyang Shi. Research on Aerodynamic Performance of J-type Blade Vertical Axis Wind Turbine. In *2020 Chinese Control And Decision Conference (CCDC)*, pages 5454–5459, Hefei, China, aug 2020. IEEE. ISBN 978-1-7281-5855-6. doi: 10.1109/CCDC49329.2020.9164408. URL https://ieeexplore.ieee.org/document/9164408/.

[75] Wen-Tong Chong, Wan Khairul Muzammil, Kok-Hoe Wong, Chin-Tsan Wang, Mohammed Gwani, Yung-Jeh Chu, and Sin-Chew Poh. Cross axis wind turbine: Pushing the limit of wind turbine technology with complementary design. *Applied Energy*, 207:78–95, dec 2017. ISSN 0306-2619. doi: 10.1016/J.APENERGY.2017.06.099. URL https://www.sciencedirect.com/science/article/pii/S030626191730853X.

[76] Wen-Tong Chong, Wan Khairul Muzammil, Hwai-Chyuan Ong, Kamaruzzaman Sopian, Mohammed Gwani, Ahmad Fazlizan, and Sin-Chew Poh. Performance analysis of the deflector integrated cross axis wind turbine. *Renewable Energy*, 138:675–690, aug 2019. ISSN 0960-1481. doi: 10.1016/J.RENENE.2019.02.005. URL https://www.sciencedirect.com/science/article/pii/S0960148119301491?via{\%}3Dihub.

[77] Wei-Cheng Wang, Wen Tong Chong, and Tien-Hsin Chao. Performance analysis of a cross-axis wind turbine from wind tunnel experiments. *Journal of Wind Engineering and Industrial Aerodynamics*,

174:312–329, mar 2018. ISSN 0167-6105. doi: 10.1016/J.JWEIA.2018.01.023. URL https://www.sciencedirect.com/science/article/pii/S0167610517304270{\#}bib5.

[78] Manabu Takao, Hideki Kuma, Takao Maeda, Yasunari Kamada, Michiaki Oki, and Atsushi Minoda. A straight-bladed vertical axis wind turbine with a directed guide vane row — Effect of guide vane geometry on the performance —. *Journal of Thermal Science*, 18(1):54–57, mar 2009. ISSN 1003-2169. doi: 10.1007/s11630-009-0054-0. URL http://link.springer.com/10.1007/s11630-009-0054-0.

[79] Rosario Nobile, Maria Vahdati, Janet F. Barlow, and Anthony Mewburn-Crook. Unsteady flow simulation of a vertical axis augmented wind turbine: A two-dimensional study. *Journal of Wind Engineering and Industrial Aerodynamics*, 125:168–179, feb 2014. ISSN 0167-6105. doi: 10.1016/J.JWEIA.2013.12.005. URL https://www.sciencedirect.com/science/article/pii/S0167610513002808.

[80] S. Zanforlin and S. Letizia. Improving the Performance of Wind Turbines in Urban Environment by Integrating the Action of a Diffuser with the Aerodynamics of the Rooftops. *Energy Procedia*, 82:774–781, dec 2015. ISSN 1876-6102. doi: 10.1016/J.EGYPRO.2015.11.810. URL https://www.sciencedirect.com/science/article/pii/S1876610215025709.

[81] Benjamin Strom, Steven L. Brunton, and Brian Polagye. Intracycle angular velocity control of cross-flow turbines. *Nature Energy*, 2(8):17103, aug 2017. ISSN 2058-7546. doi: 10.1038/nenergy.2017.103. URL http://www.nature.com/articles/nenergy2017103.

[82] G Mosetti, C Poloni, and B Diviacco. Optimization of wind turbine positioning in large windfarms by means of a genetic algorithm. Technical report, 1994. URL https://ac.els-cdn.com/0167610594900809/1-s2.0-0167610594900809-main.pdf?{_}tid=d003e3a8-7235-425f-bb95-ebd8387e4782{\&}acdnat=1540376683{_}cf1aaf46fe14c2a9b150e36231fe4f44.

[83] Johan Meyers and Charles Meneveau. Optimal turbine spacing in fully developed wind farm boundary layers. *Wind Energy*, 15(2):305–317,

mar 2012. ISSN 10954244. doi: 10.1002/we.469. URL http://doi.wiley.com/10.1002/we.469.

[84] Abdullah Mobin Chowdhury, Hiromichi Akimoto, and Yutaka Hara. Comparative CFD analysis of Vertical Axis Wind Turbine in upright and tilted configuration. *Renewable Energy*, 85:327–337, jan 2016. ISSN 0960-1481. doi: 10.1016/J.RENENE.2015.06.037. URL https://www.sciencedirect.com/science/article/pii/S096014811530063X.

[85] Mojtaba Ahmadi-Baloutaki, Rupp Carriveau, and David S-K. Ting. A wind tunnel study on the aerodynamic interaction of vertical axis wind turbines in array configurations. *Renewable Energy*, 96:904–913, oct 2016. ISSN 0960-1481. doi: 10.1016/J.RENENE.2016.05.060. URL https://www.sciencedirect.com/science/article/pii/S0960148116304700?via{\%}3Dihub.

[86] Stefania Zanforlin and Takafumi Nishino. Fluid dynamic mechanisms of enhanced power generation by closely spaced vertical axis wind turbines. *Renewable Energy*, 99:1213–1226, dec 2016. ISSN 18790682. doi: 10.1016/j.renene.2016.08.015. URL https://linkinghub.elsevier.com/retrieve/pii/S0960148116307169.

[87] Stefania Zanforlin. Advantages of vertical axis tidal turbines set in close proximity: A comparative CFD investigation in the English Channel. *Ocean Engineering*, 156:358–372, may 2018. ISSN 0029-8018. doi: 10.1016/J.OCEANENG.2018.03.035. URL https://www.sciencedirect.com/science/article/pii/S0029801818303007.

[88] H.F. Lam and H.Y. Peng. Measurements of the wake characteristics of co- and counter-rotating twin H-rotor vertical axis wind turbines. *Energy*, 131:13–26, jul 2017. ISSN 0360-5442. doi: 10.1016/J.ENERGY.2017.05.015. URL https://www.sciencedirect.com/science/article/pii/S0360544217307600?via{\%}3Dihub.

[89] D De Tavernier, C Ferreira, A Li, U S Paulsen, and H A Madsen. Towards the understanding of vertical-axis wind turbines in double-rotor configuration. Towards the understanding of vertical-axis wind turbines in double-rotor configuration. page 22015, 2018. doi: 10.1088/1742-6596/1037/2/022015. URL https://iopscience.iop.org/article/10.1088/1742-6596/1037/2/022015/pdf.

[90] Simone Giorgetti, Giulio Pellegrini, and Stefania Zanforlin. CFD Investigation on the Aerodynamic Interferences between Medium-solidity Darrieus Vertical Axis Wind Turbines. *Energy Procedia*, 81:227–239, dec 2015. ISSN 1876-6102. doi: 10.1016/J.EGYPRO.2015.12.089. URL https://www.sciencedirect.com/science/article/pii/S1876610215027381.

[91] Ian D. Brownstein, Nathaniel J. Wei, and John O. Dabiri. Aerodynamically Interacting Vertical-Axis Wind Turbines: Performance Enhancement and Three-Dimensional Flow. *Energies*, 12(14):2724, 2019. doi: 10.3390/en12142724.

[92] Sadra Sahebzadeh, Abdolrahim Rezaeiha, and Hamid Montazeri. Towards optimal layout design of vertical-axis wind-turbine farms: Double rotor arrangements. *Energy Conversion and Management*, 226:113527, dec 2020. ISSN 01968904. doi: 10.1016/j.enconman.2020.113527.

[93] Andrew Barnes and Ben Hughes. Determining the impact of VAWT farm configurations on power output. *Renewable Energy*, may 2019. ISSN 0960-1481. doi: 10.1016/J.RENENE.2019.05.084. URL https://www.sciencedirect.com/science/article/pii/S0960148119307578?via{\%}3Dihub.

[94] Robert W Whittlesey, Sebastian Liska, and John O Dabiri. Fish schooling as a basis for vertical axis wind turbine farm design. *Bioinspiration & Biomimetics*, 5(3):035005, sep 2010. ISSN 1748-3182. doi: 10.1088/1748-3182/5/3/035005. URL http://stacks.iop.org/1748-3190/5/i=3/a=035005?key=crossref.3e31f225af7e940fb723c9b14cf755bc.

[95] John O Dabiri. Potential order-of-magnitude enhancement of wind farm power density via counter-rotating vertical-axis wind turbine arrays. 2011. doi: 10.1063/1.3608170. URL http://jrse.aip.org/about/rights{_}and{_}permissions.

[96] Seyed Hossein Hezaveh, Elie Bou-Zeid, John Dabiri, Matthias Kinzel, Gerard Cortina, and Luigi Martinelli. Increasing the Power Production of Vertical-Axis Wind-Turbine Farms Using Synergistic Clustering.

Boundary-Layer Meteorology, 169(2):275–296, nov 2018. ISSN 0006-8314. doi: 10.1007/s10546-018-0368-0. URL http://link.springer.com/10.1007/s10546-018-0368-0.

[97] Ammar Naseem, Zaib Ali, and Emad Uddin. On Power Augmentation of VAWT in the wake of a bluff body. In *Proceedings of the 6th International Conference of Fluid Flow, Heat and Mass Transfer (FFHMT'19)*, page 108, Ottawa, Canada, 2019. doi: 10.11159/ffhmt19.108.

[98] H.Y. Peng, Z.D. Han, H.J. Liu, K. Lin, and H.F. Lam. Assessment and optimization of the power performance of twin vertical axis wind turbines via numerical simulations. *Renewable Energy*, 147:43–54, mar 2020. ISSN 09601481. doi: 10.1016/j.renene.2019.08.124.

[99] Aaron S. Alexander and Arvind Santhanakrishnan. Mechanisms of power augmentation in two side-by-side vertical axis wind turbines. *Renewable Energy*, 148:600–610, apr 2020. ISSN 18790682. doi: 10.1016/j.renene.2019.10.149.

[100] Galih Bangga, Amgad Dessoky, Zhenlong Wu, Krzysztof Rogowski, and Martin O.L. Hansen. Accuracy and consistency of CFD and engineering models for simulating vertical axis wind turbine loads. *Energy*, 206:118087, jun 2020. ISSN 03605442. doi: 10.1016/j.energy.2020.118087. URL https://linkinghub.elsevier.com/retrieve/pii/S0360544220311944.

[101] Mazharul Islam, David S.K. Ting, and Amir Fartaj. Aerodynamic models for Darrieus-type straight-bladed vertical axis wind turbines. *Renewable and Sustainable Energy Reviews*, 12(4):1087–1109, may 2008. ISSN 13640321. doi: 10.1016/j.rser.2006.10.023.

[102] Xin Jin, Gaoyuan Zhao, KeJun Gao, and Wenbin Ju. Darrieus vertical axis wind turbine: Basic research methods. *Renewable and Sustainable Energy Reviews*, 42:212–225, feb 2015. ISSN 1364-0321. doi: 10.1016/J.RSER.2014.10.021. URL https://www.sciencedirect.com/science/article/pii/S1364032114008387.

[103] Amin A Mohammed, Hassen M Ouakad, Ahmet Z Sahin, and Haitham M S Bahaidarah. Vertical Axis Wind Turbine Aerodynamics: Summary and Review of Momentum Models. *Journal of Energy Resources Technology*, 141:050801–1, 2019. doi: 10.1115/1.4042643.

[104] Alessandro Bianchini, Lorenzo Ferrari, and Sandro Magnani. Start-Up Behavior of a Three-Bladed H-Darrieus VAWT: Experimental and Numerical Analysis. In *ASME Turbo Expo 2011*, 2011. URL https://asmedigitalcollection.asme.org/GT/proceedings-abstract/GT2011/54617/811/351109.

[105] A. Rossetti and G. Pavesi. Comparison of different numerical approaches to the study of the H-Darrieus turbines start-up. *Renewable Energy*, 50:7–19, feb 2013. ISSN 0960-1481. doi: 10.1016/J.RENENE.2012.06.025. URL https://www.sciencedirect.com/science/article/pii/S096014811200376X{\#}bib14.

[106] Andrés Meana-Fernández, Irene Solís-Gallego, Jesús Manuel Fernández Oro, Katia María Argüelles Díaz, and Sandra Velarde-Suárez. Parametrical evaluation of the aerodynamic performance of vertical axis wind turbines for the proposal of optimized designs. *Energy*, 147: 504–517, mar 2018. ISSN 0360-5442. doi: 10.1016/J.ENERGY.2018.01.062. URL https://www.sciencedirect.com/science/article/pii/S036054421830080X?via{\%}3Dihub{\#}bib52.

[107] Sina Shamsoddin and Fernando Porté-Agel. Large eddy simulation of vertical axis wind turbine wakes. *Energies*, 7(2):890–912, 2014. ISSN 19961073. doi: 10.3390/en7020890.

[108] J. H. Strickland, B. T. Webster, and T. Nguyen. A Vortex Model of the Darrieus Turbine: An Analytical and Experimental Study. *Journal of Fluids Engineering*, 101(4):500, dec 1979. ISSN 00982202. doi: 10.1115/1.3449018. URL http://fluidsengineering.asmedigitalcollection.asme.org/article.aspx?articleid=1424807.

[109] D. Vandenberghe and E. Dick. A free vortex simulation method for the straight bladed vertical axis wind turbine. *Journal of Wind Engineering and Industrial Aerodynamics*, 26(3):307–324, jan 1987. ISSN 01676105. doi: 10.1016/0167-6105(87)90002-X. URL https://linkinghub.elsevier.com/retrieve/pii/016761058790002X.

[110] A. C. Mandal and J. D. Burton. Effects of dynamic stall and flow curvature on the aerodynamics of Darrieus turbines applying the cascade model. *Wind Engineering*, 18(6):267–282, 1994. ISSN 0309524X.

[111] Frank Scheurich and Richard E Brown. Effect of Dynamic Stall on the Aerodynamics of Vertical-Axis Wind Turbines. 2011. doi: 10.2514/1.J051060. URL http://arc.aiaa.org.

[112] David Marten, Georgios Pechlivanoglou, Christian Navid Nayeri, and Christian Oliver Paschereit. Nonlinear Lifting Line Theory Applied to Vertical Axis Wind Turbines: Development of a Practical Design Tool. *Journal of Fluids Engineering*, 140 (2), feb 2018. ISSN 0098-2202. doi: 10.1115/1.4037978. URL https://asmedigitalcollection.asme.org/fluidsengineering/article/doi/10.1115/1.4037978/374177/Nonlinear-Lifting-Line-Theory-Applied-to-Vertical.

[113] E Tingey and A Ning. Parameterized Vertical-Axis Wind Turbine Wake Model Using CFD Vorticity Data. *ASME Wind Energy Symposium*, 2016. doi: 10.2514/6.2016-1730. URL https://scholarsarchive.byu.edu/facpub.

[114] Richard E. Brown. Rotor Wake Modeling for Flight Dynamic Simulation of Helicopters. *AIAA Journal*, 38(1):57–63, jan 2000. ISSN 0001-1452. doi: 10.2514/2.922. URL http://arc.aiaa.org/doi/10.2514/2.922.

[115] M. Sergio Campobasso, Jernej Drofelnik, and Fabio Gigante. Comparative assessment of the harmonic balance Navier–Stokes technology for horizontal and vertical axis wind turbine aerodynamics. *Computers & Fluids*, 136:354–370, sep 2016. ISSN 0045-7930. doi: 10.1016/J.COMPFLUID.2016.06.023. URL https://www.sciencedirect.com/science/article/pii/S0045793016302080.

[116] Marco Raciti Castelli, Guido Ardizzon, Lorenzo Battisti, Ernesto Benini, and Giorgio Pavesi. Modeling Strategy and Numerical Validation for a Darrieus Vertical Axis Micro-Wind Turbine. In *Volume 7: Fluid Flow, Heat Transfer and Thermal Systems, Parts A and B*, pages 409–418. ASME, jan 2010. ISBN 978-0-7918-4444-1. doi: 10.1115/IMECE2010-39548. URL http://proceedings.asmedigitalcollection.asme.org/proceeding.aspx?articleid=1616421.

[117] A Orlandi, M Collu, S Zanforlin, and A Shires. 3D URANS Analysis of a Vertical Axis Wind Turbine in Skewed Flows. 2015. ISSN 0167-6105. doi: 10.1016/j.jweia.2015.09.010. URL http://eprints.whiterose.ac.uk/95027/http://creativecommons.org/licenses/by-nc-nd/4.0/eprints@whiterose.ac.ukhttps://eprints.whiterose.ac.uk/.

[118] Chao Li, Songye Zhu, You-lin Xu, and Yiqing Xiao. 2.5D large eddy simulation of vertical axis wind turbine in consideration of high angle of attack flow. *Renewable Energy*, 51:317–330, mar 2013. ISSN 0960-1481. doi: 10.1016/J.RENENE.2012.09.011. URL https://www.sciencedirect.com/science/article/pii/S0960148112005770.

[119] Jiao He, Xin Jin, Shuangyi Xie, Le Cao, Yaming Wang, Y. Lin, and Ning Wang. CFD modeling of varying complexity for aerodynamic analysis of H-vertical axis wind turbines. *Renewable Energy*, 145:2658–2670, jan 2020. ISSN 18790682. doi: 10.1016/j.renene.2019.07.132.

[120] Antonio Posa, Colin M. Parker, Megan C. Leftwich, and Elias Balaras. Wake structure of a single vertical axis wind turbine. *International Journal of Heat and Fluid Flow*, 61:75–84, oct 2016. ISSN 0142-727X. doi: 10.1016/J.IJHEATFLUIDFLOW.2016.02.002. URL https://www.sciencedirect.com/science/article/pii/S0142727X16300285?via{\%}3Dihub.

[121] Hang Lei, Dai Zhou, Yan Bao, Ye Li, and Zhaolong Han. Three-dimensional Improved Delayed Detached Eddy Simulation of a two-bladed vertical axis wind turbine. *Energy Conversion and Management*, 133:235–248, feb 2017. ISSN 0196-8904. doi: 10.1016/J.ENCONMAN.2016.11.067. URL https://www.sciencedirect.com/science/article/pii/S0196890416310767?via{\%}3Dihub.

[122] Yutaka Hara, Naoki Horita, Shigeo Yoshida, Hiromichi Akimoto, and Takahiro Sumi. Numerical Analysis of Effects of Arms with Different Cross-Sections on Straight-Bladed Vertical Axis Wind Turbine. *Energies*, 12(11):2106, jun 2019. ISSN 1996-1073. doi: 10.3390/en12112106. URL https://www.mdpi.com/1996-1073/12/11/2106.

[123] H.F. Lam and H.Y. Peng. Study of wake characteristics of a vertical axis wind turbine by two- and three-dimensional computational

fluid dynamics simulations. *Renewable Energy*, 90:386–398, may 2016. ISSN 09601481. doi: 10.1016/j.renene.2016.01.011. URL https://linkinghub.elsevier.com/retrieve/pii/S0960148116300118.

[124] G. Tescione, D. Ragni, C. He, C.J. Simão Ferreira, and G.J.W. van Bussel. Near wake flow analysis of a vertical axis wind turbine by stereoscopic particle image velocimetry. *Renewable Energy*, 70: 47–61, oct 2014. ISSN 0960-1481. doi: 10.1016/J.RENENE.2014.02.042. URL https://www.sciencedirect.com/science/article/pii/S0960148114001335.

[125] Abdolrahim Rezaeiha, H. Montazeri, and Bert Blocken. CFD analysis of dynamic stall on vertical axis wind turbines using Scale-Adaptive Simulation (SAS): Comparison against URANS and hybrid RANS/LES. *Energy Conversion and Management*, 196:1282–1298, sep 2019. ISSN 01968904. doi: 10.1016/j.enconman.2019.06.081.

[126] Abdolrahim Rezaeiha, Hamid Montazeri, and Bert Blocken. On the accuracy of turbulence models for CFD simulations of vertical axis wind turbines. *Energy*, 180:838–857, aug 2019. ISSN 0360-5442. doi: 10.1016/J.ENERGY.2019.05.053. URL https://www.sciencedirect.com/science/article/pii/S0360544219309168?via{\%}3Dihub.

[127] Abdolrahim Rezaeiha, Ivo Kalkman, and Bert Blocken. CFD simulation of a vertical axis wind turbine operating at a moderate tip speed ratio: Guidelines for minimum domain size and azimuthal increment. *Renewable Energy*, 107:373–385, jul 2017. ISSN 0960-1481. doi: 10.1016/J.RENENE.2017.02.006. URL https://www.sciencedirect.com/science/article/pii/S0960148117300848.

[128] Abdolrahim Rezaeiha, Hamid Montazeri, and Bert Blocken. Towards accurate CFD simulations of vertical axis wind turbines at different tip speed ratios and solidities: Guidelines for azimuthal increment, domain size and convergence. *Energy Conversion and Management*, 156:301–316, jan 2018. ISSN 0196-8904. doi: 10.1016/J.ENCONMAN.2017.11.026. URL https://www.sciencedirect.com/science/article/pii/S0196890417310786?via{\%}3Dihub.

[129] László Daróczy, Gábor Janiga, Klaus Petrasch, Michael Webner, and Dominique Thévenin. Comparative analysis of turbulence models

for the aerodynamic simulation of H-Darrieus rotors. *Energy*, 90: 680–690, oct 2015. ISSN 0360-5442. doi: 10.1016/J.ENERGY.2015.07.102. URL https://www.sciencedirect.com/science/article/pii/S0360544215009974?via{\%}3Dihub{\#}bib17.

[130] Louis Angelo Danao, Jonathan Edwards, Okeoghene Eboibi, and Robert Howell. A numerical investigation into the influence of unsteady wind on the performance and aerodynamics of a vertical axis wind turbine. *Applied Energy*, 116:111–124, mar 2014. ISSN 0306-2619. doi: 10.1016/J.APENERGY.2013.11.045. URL https://www.sciencedirect.com/science/article/pii/S0306261913009513?via{\%}3Dihub{\#}b0045.

[131] P. J. Roache. Perspective: A method for uniform reporting of grid refinement studies. *Journal of Fluids Engineering, Transactions of the ASME*, 116(3):405–413, sep 1994. ISSN 1528901X. doi: 10.1115/1.2910291.

[132] K. M. Almohammadi, D. B. Ingham, L. Ma, and M. Pourkashanian. Effect of Transitional Turbulence Modelling on a Straight Blade Vertical Axis Wind Turbine. In *Alternative Energies: Updates on Progress*, pages 93–112. Springer, Berlin, Heidelberg, 2013. doi: 10.1007/978-3-642-40680-5_5. URL http://link.springer.com/10.1007/978-3-642-40680-5{_}5.

[133] R Bravo, S Tullis, and S Ziada. Performance testing of a small vertical-axis wind turbine. *21st Canadian Congress of Applied ...*, (June 2007):2–3, 2007. URL http://www.eng.mcmaster.ca/{~}stullis/index{_}files/BravoCANCAM2007.pdf.

[134] Rosario Lanzafame, Stefano Mauro, and Michele Messina. 2D CFD Modeling of H-Darrieus Wind Turbines Using a Transition Turbulence Model. *Energy Procedia*, 45:131–140, jan 2014. ISSN 1876-6102. doi: 10.1016/J.EGYPRO.2014.01.015. URL https://www.sciencedirect.com/science/article/pii/S1876610214000162?via{\%}3Dihub.

[135] Francesco Balduzzi, Alessandro Bianchini, Riccardo Maleci, Giovanni Ferrara, and Lorenzo Ferrari. Critical issues in the CFD

simulation of Darrieus wind turbines. *Renewable Energy*, 85:419–435, jan 2016. ISSN 0960-1481. doi: 10.1016/J.RENENE.2015.06.048. URL https://www.sciencedirect.com/science/article/pii/S0960148115300719?via{\%}3Dihub.

[136] K.M. Almohammadi, D.B. Ingham, L. Ma, and M. Pourkashan. Computational fluid dynamics (CFD) mesh independency techniques for a straight blade vertical axis wind turbine. *Energy*, 58:483–493, sep 2013. ISSN 0360-5442. doi: 10.1016/J.ENERGY.2013.06.012. URL https://www.sciencedirect.com/science/article/pii/S0360544213005100.

[137] Abdolrahim Rezaeiha, Ivo Kalkman, and Bert Blocken. CFD simulation of a vertical axis wind turbine operating at a moderate tip speed ratio: Guidelines for minimum domain size and azimuthal increment. *Renewable Energy*, 107:373–385, jul 2017. ISSN 0960-1481. doi: 10.1016/J.RENENE.2017.02.006. URL https://www.sciencedirect.com/science/article/pii/S0960148117300848.

[138] F. Trivellato and M. Raciti Castelli. On the Courant–Friedrichs–Lewy criterion of rotating grids in 2D vertical-axis wind turbine analysis. *Renewable Energy*, 62:53–62, feb 2014. ISSN 09601481. doi: 10.1016/j.renene.2013.06.022. URL https://linkinghub.elsevier.com/retrieve/pii/S0960148113003157.

[139] Ian D. Brownstein, Matthias Kinzel, and John O. Dabiri. Performance enhancement of downstream vertical-axis wind turbines. *Journal of Renewable and Sustainable Energy*, 8(5):053306, sep 2016. ISSN 1941-7012. doi: 10.1063/1.4964311. URL http://aip.scitation.org/doi/10.1063/1.4964311.

[140] P. Schito, I. Bayati, M. Belloli, L. Bernini, V. Dossena, and A. Zasso. Numerical Wind Tunnel Tests of an Open Data IPC-VAWT. Technical report, 2018. URL http://link.springer.com/10.1007/978-3-319-74944-0{_}8.

[141] Haiying Sun, Xiaoxia Gao, and Hongxing Yang. A review of full-scale wind-field measurements of the wind-turbine wake effect and a

measurement of the wake-interaction effect. *Renewable and Sustainable Energy Reviews*, 132:110042, oct 2020. ISSN 18790690. doi: 10.1016/j.rser.2020.110042.

[142] British Standards. Wind Turbine—Part 1: Design Requirements, IEC 61400-1. Technical report, 2005. URL https://scholar.google.co.uk/scholar?hl=en{\&}as{_}sdt=0,5{\&}q=IEC+61400-1{\#}1.

[143] Vincent F-C. Rolin and Fernando Porté-Agel. Experimental investigation of vertical-axis wind-turbine wakes in boundary layer flow. *Renewable Energy*, 118:1–13, apr 2018. ISSN 0960-1481. doi: 10.1016/J.RENENE.2017.10.105. URL https://www.sciencedirect.com/science/article/pii/S0960148117310753?via{\%}3Dihub.

[144] Alexandrina Untaroiu, Houston G. Wood, Paul E. Allaire, and Robert J. Ribando. Investigation of Self-Starting Capability of Vertical Axis Wind Turbines Using a Computational Fluid Dynamics Approach. *Journal of Solar Energy Engineering*, 133(4): 041010, nov 2011. ISSN 01996231. doi: 10.1115/1.4004705. URL http://solarenergyengineering.asmedigitalcollection.asme.org/article.aspx?articleid=1458709.

[145] Zhenlong Wu, Galih Bangga, and Yihua Cao. Effects of lateral wind gusts on vertical axis wind turbines. *Energy*, 167:1212–1223, jan 2019. ISSN 03605442. doi: 10.1016/j.energy.2018.11.074.